Characterization and Response of Thermoplastic Composites and Constituents

Pierce David Umberger

Thesis submitted to the Faculty of the
Virginia Polytechnic Institute and State University
in partial fulfillment of the requirements for the degree of

Master of Science
in
Engineering Mechanics

Scott W. Case, Chair
Michael W. Hyer
Romesh C. Batra

June 1, 2010
Blacksburg, Virginia

Keywords: UHMWPE, Time-temperature superposition, composite materials

Characterization and Response of Thermoplastic Composites and Constituents

Pierce David Umberger

ABSTRACT

The research presented herein is an effort to support computational modeling of ultra-high molecular weight polyethylene (UHMWPE) composites. An effort is made to characterize the composites and their constituents. UHMWPE, as a polymer, is time and temperature dependent. Using time-temperature superposition (tTSP), the constituent properties are studied as a function of strain rate. Properties that are believed to be significant are fiber tensile properties as a function of strain rate, as well as the through-thickness shear behavior of composite laminates. Obtaining fiber properties proved to be a challenge. The high strength and low surface energy of the fibers makes gripping specimens difficult. Several different methods of fixturing and gripping are investigated, eventually leading to a combination of friction and adhesion approaches where a fiber was wrapped on an adhesive coated cardboard mandrel and then gripped in the test fixture. Fiber strength is estimated using tTSP to equivalent strain rates approaching 10^6 sec^{-1}. Punch-shear testing of UHMWPE laminates is conducted at quasi-static strain rates and the dependence of the results on thickness and test geometry is investigated.

Acknowledgments

The author would like to thank the following people for helping make this work possible:

- Dr. Scott W. Case for the opportunity to study these problems, and for his advice and support along the way.
- Drs. Michael W. Hyer and Romesh C. Batra for willingly sharing their knowledge and advice.
- Honeywell Advanced Materials, especially Lori Wagner, David Hurst, Ashok Bhatnagar, Henry Ardiff, Brian Waring, and Brian Arvidson for supplying the Spectra fiber and SpectraShield materials for this study, in addition to the offering of technical expertise and assistance in sample fabrication.
- Army Research Lab, especially Michael Maher, James Wolbert, and Bryan Love for the offering of technical expertise and financial support of this work, along with assistance in sample fabrication.
- Lisa Smith and Beverly Williams for taking care of the work behind the scenes for which I am greatly in debt.
- David Simmons, and Darryl Link for fabrication of the jigs used in much of the experimental testing.
- My fellow MRG students for the conversations, advice, and friendship. It is a privilege working with you.
- My parents, David and Christina Umberger, and brother Dillon Umberger for their tremendous moral and financial support during the (still) ongoing years of my education.
- My fiancée, Betsy Thompson, for her constant love, support, and – most importantly – patience. There is nothing more I could possibly wish for.

Research was sponsored by the Army Research Laboratory and was accomplished under Cooperative Agreement Number W911NF-06-2-0014. The views and conclusions contained in this document are those of the authors and should not be interpreted as representing official policies, either expressed or implied, of the Army Research Laboratory or the U.S. Government. The U.S. Government is authorized to reproduce and distribute reprints for Government purposes notwithstanding any copyright notation heron.

Contents

List of Figures

List of Tables

Attribution

The content of this paper is the original work of Pierce David Umberger. In Chapter 2, Figures 2.1, 2.2, 2.3, 2.4 are the work of their respective authors and are reprinted with permission. The data presented in Figure 2.16 is the work of Frederick Cook. All other figures are the work of the author.

Chapter 1

Introduction

Ultra-high molecular weight polyethylene (UHMWPE) composites are used extensively in lightweight armor applications. Its high strength and stiffness and light weight make it a natural choice for this role. UHMWPE has been shown to exhibit increased stiffness and strength with increased strain rate [1], [4]. During ballistic impact, strain rates on the order of 10^5 sec^{-1} are typical. The primary goal of the UHMWPE fiber testing was to enable modeling at the composite level at high strain rates (model more, shoot less). Therefore, fiber tensile properties are desired at strain rates approaching 10^5 sec^{-1}. Such strain rates are difficult to attain in a laboratory environment. Hydraulic load frames typically generate strain rates on the order of 10^1 sec^{-1}, while screw-driven load frames typically 1 order of magnitude lower. High rate test setups such the Split Hopkinson bar have been used to obtain properties in the range of interest [14], but bridging the gap between load frame strain rates and Split Hopkinson strain rates is difficult.

In Chapter 2 of this work, we attempt to estimate high strain rate properties of these materials using a low strain rate tension test. To this end, the principle of time-temperature superposition (tTSP) was invoked, utilizing calibrated shifts in temperature to correspond to changes in strain rate. This method is well established, and work published by Alcock et al. demonstrated the applicability to thermoplastic fiber composites [1]. Material variability and difficulties in sample fixturing led to significant challenges in conducting repeatable tests. Although the test data as presented in this work exhibits significant scatter, significant trends are evident with changes in temperature and strain rate and these results are considered.

Working with and testing UHMWPE fibers and composites has presented many challenges. The high strength and low surface energy of the fibers makes gripping specimens difficult. Single fibers would often pull out of their fixture before failure. Several different methods of gripping and fixturing the samples were developed, eventually coming to a combination of friction and adhesion approaches, where a fiber was wrapped on an adhesive coated cardboard mandrel and then gripped in the test fixture. The method is discussed further in Chapter 2.

Another mechanical property of particular importance, especially during impact events, is the through-thickness laminate shear behavior. A punch-shear type test fixture was designed and manufactured, consisting of a clamping die fixture with a round, 19 mm diameter hole through which a punch was driven, creating a region of intense shear at the punch-die interface. Two versions of the punch were tested, one allowing, and one preventing curvature and displacement of the laminate in the center section of the punch. Shear strength results and a discussion of the variation between nearly pure shear test configurations and those allowing membrane type laminate behavior are discussed. The material is discussed further in Chapter 3.

Both papers presented herein are scheduled for publication in various forms. Time-Temperature Superposition and High Rate Properties of UHMWPE Fibers will be combined with similar work on UHMWPE laminae and laminates and will be published at the 2010 Society of Experimental Mechanics (SEM) Annual Conference in June, 2010. Through Thickness Shear and Membrane Behavior of UHMWPE Composites will be published at the 2010 Society for the Advancement of Material and Process Engineering (SAMPE) Fall Technical Conference in October 2010.

Chapter 2

Time-Temperature Superposition and High Rate Response of UHMWPE Fibers

2.1 Abstract

The high strain rate response of ultra high molecular weight polyethylene (UHMWPE) laminae and laminates is of interest to support computational modeling of applications where impact damage may occur. In this study, the efficacy of utilizing time-temperature superposition principle (tTSP) to determine the high strain rate response of UHMWPE composites is investigated. Fiber tensile properties are measured at various temperatures and strain rates. Testing is completed at thermo-rheologically equivalent temperature-strain rate combinations to evaluate the effectiveness and limitations of the shifting approach. Analysis of failure data indicates that at the fiber level tTSP may be applicable, therefore high strain rate properties are estimated.

2.2 Introduction

UHMWPE composites are used in many applications requiring light weight and high impact strength, particularly armor applications. One of the most widely used UHMWPE material system is the Spectra/SpectraShield line, manufactured by Honeywell. One of the major applications for these material systems are lightweight ballistic armors. Work by Peijs and others found that due to the high degree of anisotropy of UHMWPE fibers and the method of composite fabrication, fiber properties largely dominate the behavior of the composite as a whole [10].

Fiber properties are a major factor controlling ballistic performance of a composite armor. Unfortunately both the size and viscoelastic nature of the fibers complicates material characterization. Gripping individual fibers or even fiber bundles is difficult without introducing stress concentrations and causing premature failure. In the case of fiber bundles, care must be taken to ensure that load is distributed evenly among all fibers [11]. Knotting or other similar methods of attachment result in considerable stress concentrations, often threefold or larger, causing premature fiber failure [14].

Bonding has been used successfully in tensile test of various fibers [5],[7],[15]. Fiber bonding must be carefully controlled, as any uneven bonding or any adhesive seepage between fibers within the gage length will result in stress concentrations during testing. Testing of single filaments rather than bundles is one solution to the inter-fiber issues associated with bonding or other gripping methods. In 2005, Feih et al. performed single filament tests on sized and unsized glass fibers using a cardboard sample fixture to which individual samples were bonded. Figure 2.1 shows the fixture used. The fiber is oriented and bonded between the holes. After curing, the center section is cut away, exposing the tabbed fiber for testing [5].

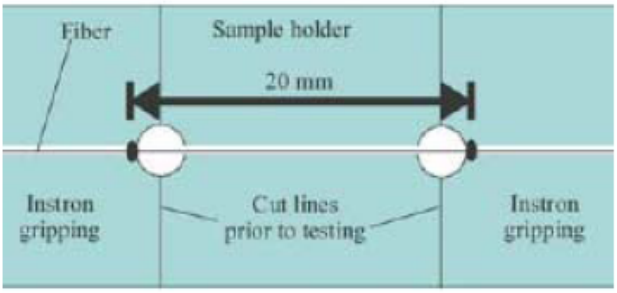

Figure 2.1: Bonding fibers to a fixture allows a gripping surface for testing without causing fiber failure at the grip location [5]. [Used with permission]

Scharfeld, et al. utilized a capstan method in which the fibers were wound on metal pegs for quasi-static testing. The capstan grips were successful in testing high strength fibers to failure without introducing stresses sufficient to cause premature fiber failure occurring at the grips. Figure 2.2 shows a diagram and photograph of an Aramid fiber test using these grips. However, the mass of the capstan grips can pose a problem for dynamic and high strain rate testing [11]. Often in dynamic testing, however, the specimen is not tested to failure, but rather at much lower stress levels. This allows other grip methods to be employed in this scenario.

Developing strain rate dependence correlation at strain rates on the same order of magnitude as ballistic impact is not possible on most test equipment. In 2006, Tan et al. used a Split Hopkinson bar setup to develop constitutive properties of Aramid fibers at high strain rates and traditional tensile test methods at quasi-static strain rates. They found that Twaron aramid fibers are strain-rate sensitive, both in constitutive properties and failure mechanism.

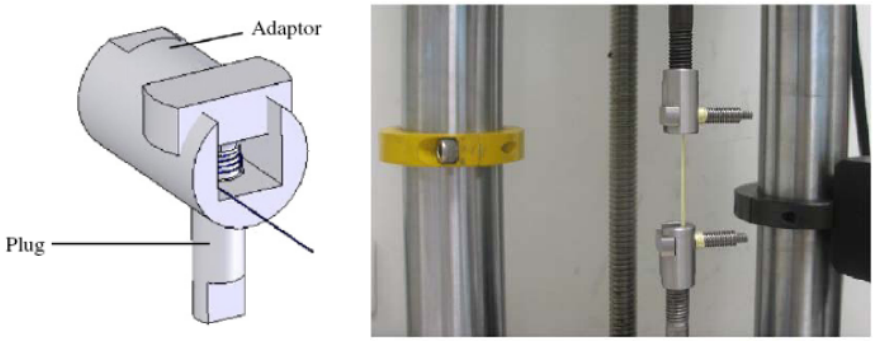

Figure 2.2: Capstan grip diagram and photograph of a quasi-static tensile test [14]. [Used with permission]

A three element linear viscoelastic model was used to correlate the viscoelastic response of the fibers to test data. Three-parameter solid models are often sufficient when fitting linear viscoelastic data over relatively few decades in log-time. Good correlation can be found within the bounds of the fit. The stress-strain behavior of the model is given as

$$(1 + \frac{K_2}{K_1})\sigma + \frac{\mu}{K_2}\dot{\sigma} = K_2\epsilon + \mu\dot{\epsilon} \tag{2.1}$$

where K_1, K_2, and μ are material properties described by Shim et al. [12], [13], σ and $\dot{\sigma}$ are the applied stress and time rate of change of stress, and ϵ and $\dot{\epsilon}$ are the strain and time rate change of strain. Available test methods leave a large gap in the strain rates that can be directly tested. As a result, viscoelastic modeling and the time-temperature superposition principle (tTSP) are often used to interpolate between these extremes.

Time-temperature superposition is based on shifting data taken at different temperatures left or right along a time scale. The master curve developed by the combination of these data can then be used to predict the behavior of the material at time scales or strain rates that are not physically achievable on test equipment [3]. The most common method for time-temperature superposition is the use of the Williams-Landel-Ferry (WLF) equation:

$$log(a_T) = \frac{-C_1(T - T_{ref})}{C_2 + (T - T_{ref})} \tag{2.2}$$

where C_1 and C_2 are empirical constants and T_{ref} is the reference temperature. If the reference temperature is chosen to be the glass transition temperature, T_g of the material, then universal values of C_1 and C_2 are 17.44 and 51.6, respectively.

In 2007, Alcock et al. investigated the effects of temperature and strain rate on the mechanical properties of highly oriented PP tapes and all-PP composites. The authors analyzed strain rate and temperature effects on tensile modulus and strength and developed master curves for each. These master curves were used to predict the constitutive behavior of the

tapes and composites at various strain rates, including those that are difficult to achieve with physical testing. Figure 2.3 shows strength vs. strain rate for several different temperatures. Figure 2.4 shows the master curve developed from the data in Figure 2.3, covering a much wider range of strain rate [1].

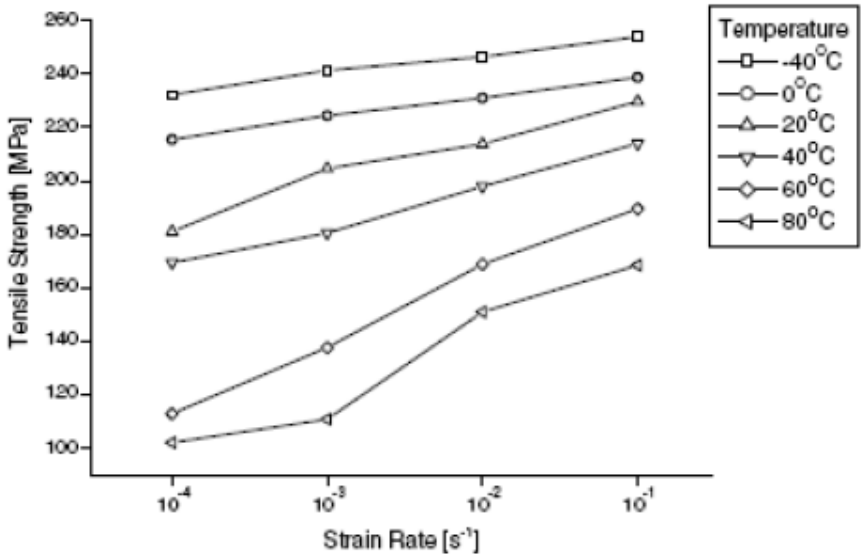

Figure 2.3: Tensile strength vs. strain rate for several temperatures. Tensile strength increases with increasing strain rate and decreasing temperature [1]. [Used with permission]

Time-temperature superposition is only directly applicable to fully amorphous polymers. However, tTSP has been applied and works well for failure mechanisms of composite systems by Miyano et al., who used tTSP to predict long-term durability in GFRP composite systems [9].

In this chapter, the temperature (and by analogy, rate dependence) of UHMWPE fiber strength is investigated, and tTSP is applied to estimate properties at high strain rate.

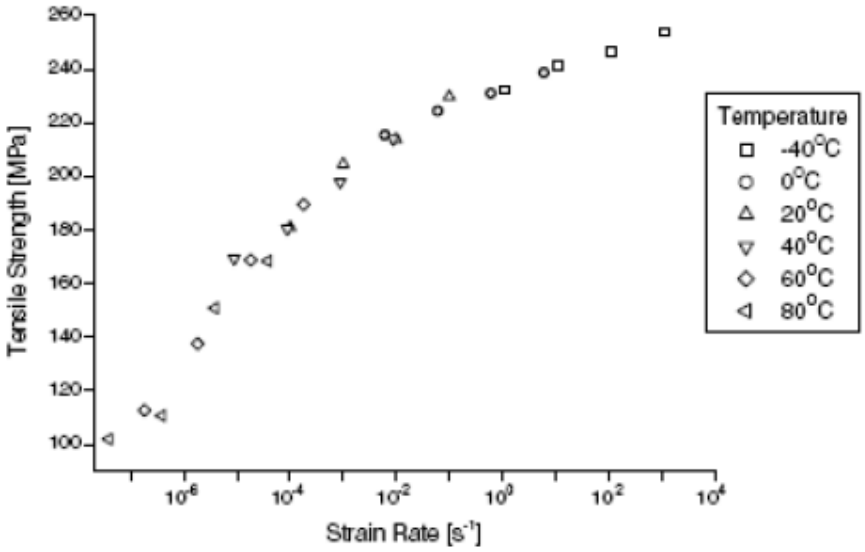

Figure 2.4: Master curve developed from the data in Figure 2.3 with a reference temperature of 20°C [1]. [Used with permission]

2.3 Sample Preparation

Spectra S1000 and S3000 fibers (supplied by Honeywell) are used. Fibers were received in tows on spools. In tow testing, there is often difficulty in loading all fibers equally. For that reason, the choice was made to test only single fibers.

2.3.1 Fiber Processing

Fibers were separated from fiber tows, as individual loose fibers were unavailable. However, the twist applied during tow manufacturing was minimal, so there was little problem in removing fibers from as-received tows. Approximately 0.5 m of fiber tow was removed from the spool and attached to a work surface with tape. Using a magnifier, razor blade, and forceps, a single fiber was severed at one end and gently removed from the tow, taking care not to cause fiber kinking or excessive bending or otherwise damage the fiber. These fibers were bonded to a glass plate for mounting.

2.3.2 Fiber Specimen Preparation

Several different fixturing methods were used. In fact, proper fiber gripping was one of the largest hurdles encountered in this research. First, fibers were bonded to cardboard tabs which were then gripped for testing, using the method of Feih et al. [5]. Figure 2.5 shows the fiber, bonded to a cardstock "frame" with a 10 mm gage length. Several adhesives were tested, including cyanoacrylate based adhesives, and 3M 4693H, a specialty adhesive designed specifically for bonding to polyethylene and polypropylene. These tab fixtures were mounted in the test fixture, and then the side portions of the "frame" were cut away, leaving the fiber sample for testing, shown in Figure 2.6

While the tabbing/bonding method has been successful for many fiber types, including glass [5], and polypropylene, the method did not work well for UHMWPE fibers. The extremely high strength, coupled with the very low surface energy of the material led to problems applying loads sufficient to cause fiber failure. In fact, approximately 90% of the fibers became debonded and pulled out of the test fixture prior to fiber failure.

As a result, the fiber gripping method was changed to a mandrel wrapping method. The individually prepared fibers were wrapped around 2 mm diameter cardboard mandrels that had been coated with 3M 4693H adhesive. Approximately 0.25 m of fiber was wrapped around each mandrel, leaving a gage length of 10 mm. The assembly was allowed to cure for 4 hours and then testing commenced.

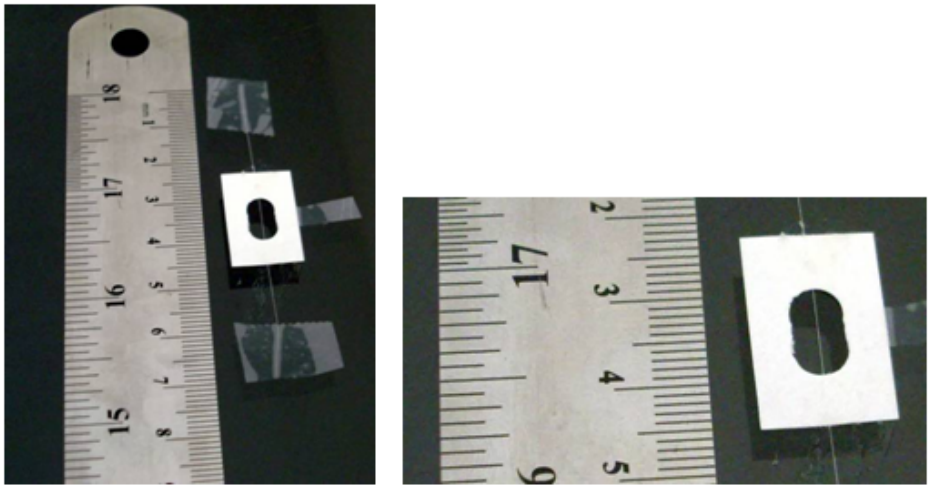

Figure 2.5: An untested tabbed/bonded fiber sample, before mounting.

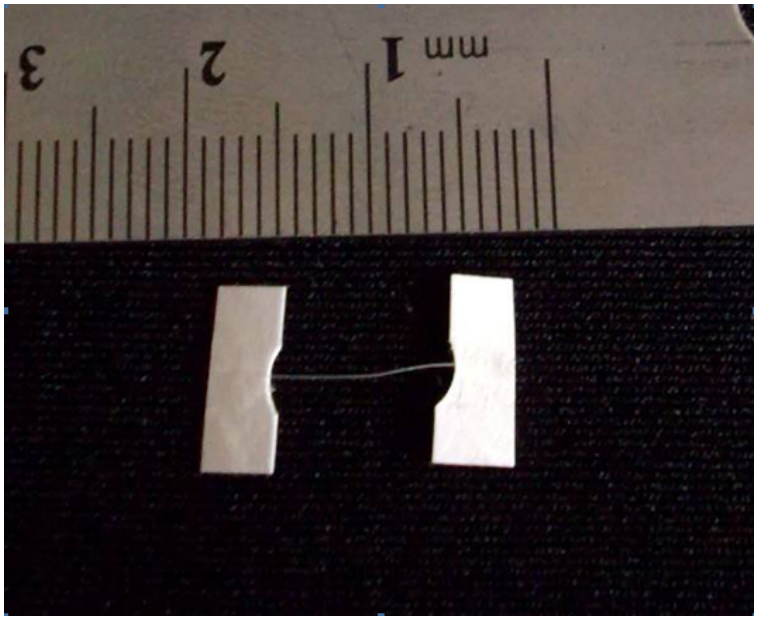

Figure 2.6: A tabbed/bonded fiber sample with the edges cut away. The sample is gripped on the white cardboard tabs.

2.4 Testing Procedure

2.4.1 Creep Compliance Testing

A TA Instruments Q800 DMA was used to conduct creep compliance tests of fibers in order to develop material master curves and shift factors. Fibers in their mandrel wrapped fixture were gripped in the DMA, clamped to a torque of 0.45 N-m, and subjected to a creep compliance test. An attached furnace and liquid nitrogen cooling chamber on the DMA allowed a temperature range of -140 °C to +500 °C with a precision of 0.1 °C. The creep compliance test program consisted of a temperature sweep from -70 °C to +40 °C in 10 °C increments. At each temperature, the chamber was held and allowed to equilibrate for 10 minutes, then a tensile load of 0.14 N (corresponding to approximately 375 MPa) was applied to the fiber and the displacement of the sample was measured for 10 minutes.

2.4.2 Fiber Tensile Testing

Fiber tensile tests were conducted using the same TA Q800 DMA as was used in creep compliance testing. Again, an attached furnace and liquid nitrogen cooling chamber allowed for a temperature range of -140 °C to +500 °C with a precision of 0.1 °C. For all tests, fibers, either bonded and tabbed, or mandrel wrapped, were gripped in the DMA film/fiber grips and torqued to 0.45 N-m. The furnace was closed and allowed to equilibrate for 10 minutes after reaching the desired set temperature. For most tests, the DMA was run in displacement control mode. The fibers were loaded at constant strain rate until failure. Tensile tests were carried out at temperatures between -100 °C and +25 °C and strain rates of $5\text{x}10^{-4}$ sec^{-1} to $5\text{x}10^{-2}$ sec^{-1}. Figure 2.7 shows a bonded/tabbed specimen gripped in the DMA film/fiber grips, while Figure 2.8 shows a mandrel wrapped specimen.

Because of the closed furnace assembly and the small diameter of the fibers (approximately 27.5 μm nominal diameter), the only indicator of strain was from crosshead displacement, as mechanical or optical extensometer methods were not feasible. Load was measured using the DMA 18 N integrated load cell.

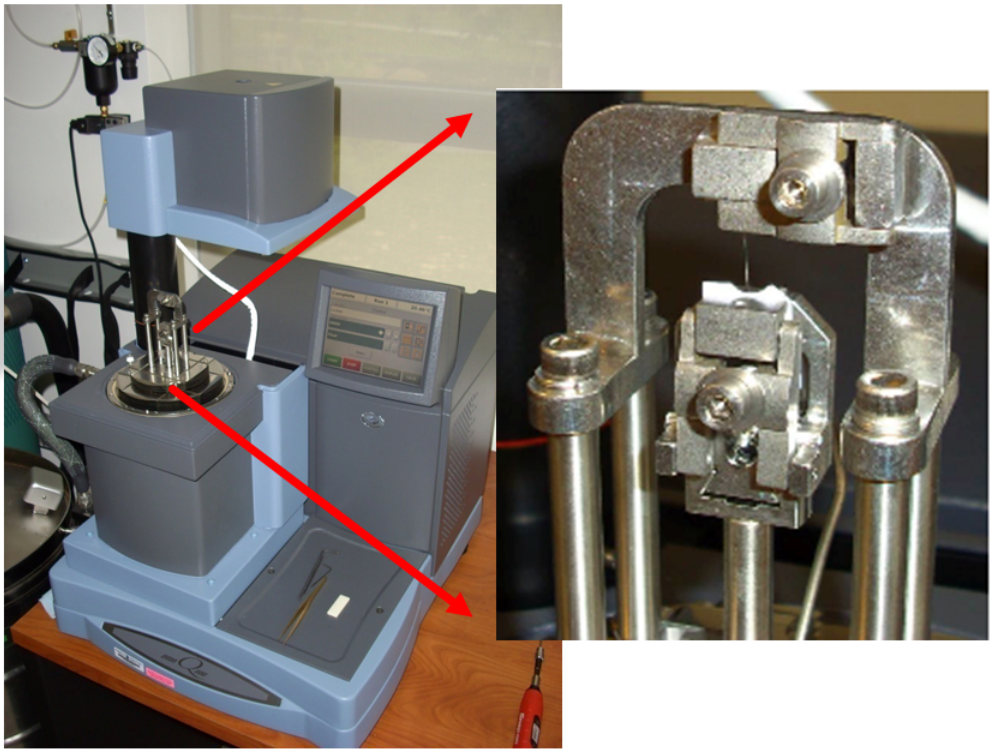

Figure 2.7: A tabbed/bonded fiber sample mounted in the Q800 DMA.

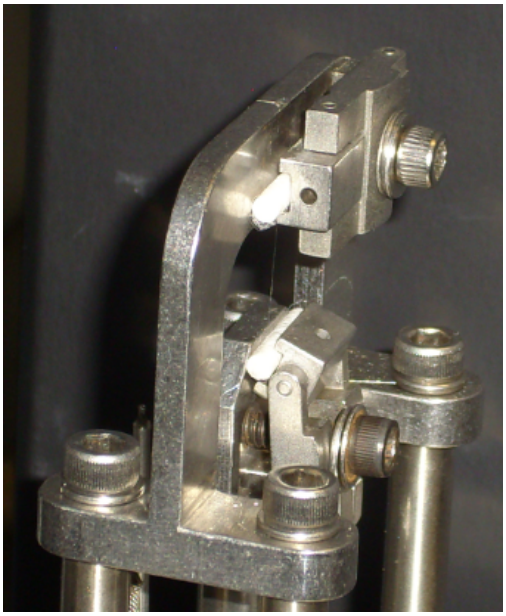

Figure 2.8: A mandrel wrapped fiber sample mounted in the Q800 DMA.

2.5 Results

The initial test plan was to develop a master curve and shift factors from tensile testing alone, shifting strength data sets left and right in time to match up sets from different temperatures. To complete this, a set of fiber tests at a wide range of temperatures and strain rates was conducted. As Figure 2.9 shows, there are visible trends in the data, but the scatter is sufficiently large, and the decades of available data are sufficiently few that constructing a master curve solely from this data set is not feasible.

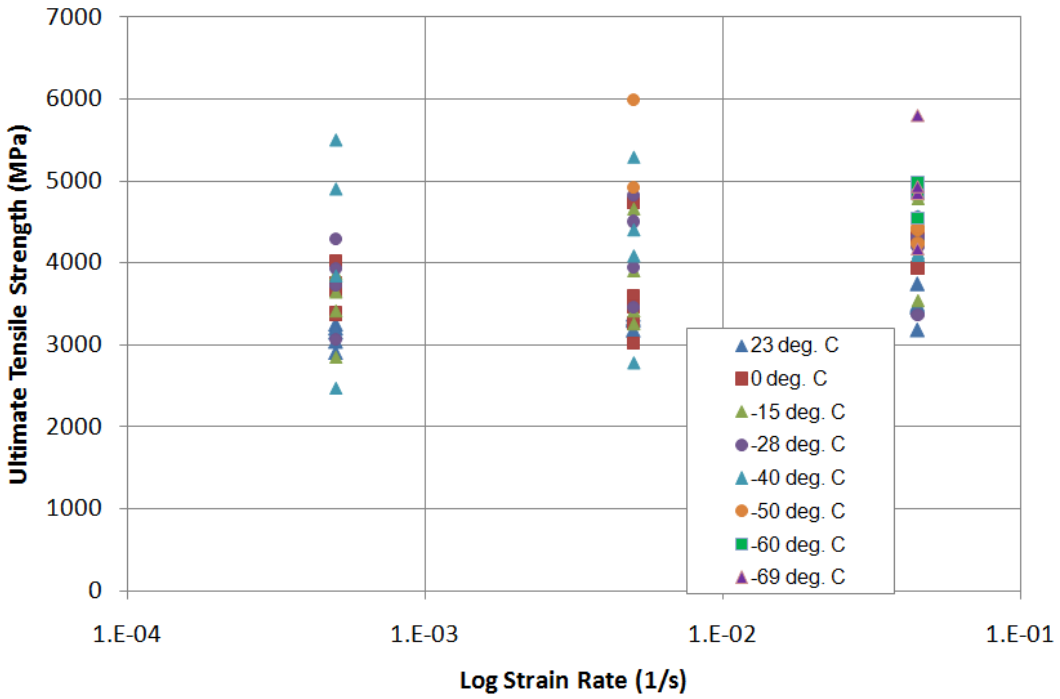

Figure 2.9: S3000 fiber stress at failure vs. strain rate at various temperatures.

In an attempt to generate meaningful fiber strength data for high strain rates, the decision was made to use fiber creep compliance data to construct a material master curve and generate shift factors, and to use these shift factors to shift fiber strength with temperature. This, of course, makes the assumption that the mechanisms that govern changes in creep compliance with time and temperature are the same mechanisms that govern tensile strength versus temperature and strain rate.

Figure 2.10 shows an unshifted plot of the S3000 fiber creep compliance data for one test run. Figure 2.11 shows the same data shifted left and right such that slopes align, and Figure 2.12 shows the corresponding shift factors for the master curve in Figure 2.11. Figures 2.11 and 2.12 are for a reference temperature T_{ref} of 20 °C

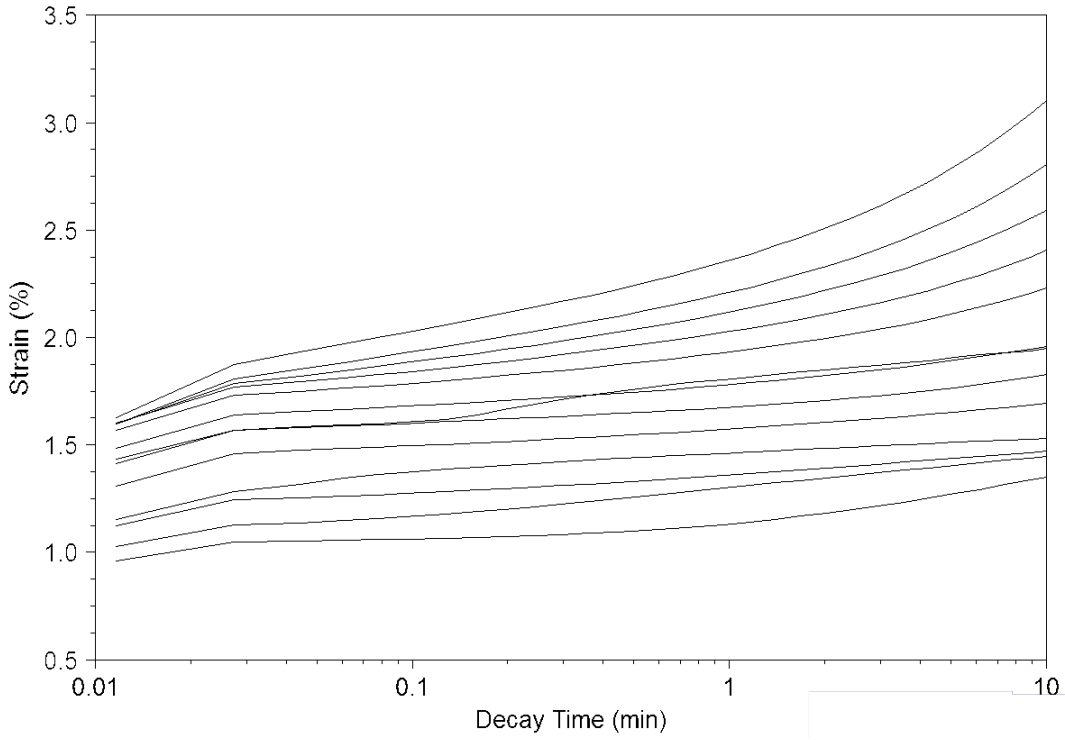

Figure 2.10: Unshifted strain for creep compliance of a S3000 fiber sample.

To help validate that the shift factors derived from creep compliance testing are applicable to tensile strength, we test three decades of "true" strain rate, and shift data sets in single decade increments. As such, we should have two decades of overlap in either direction for each data set. Figure 2.13 shows the data from Figure 2.9 shifted according to the shift factors in Figure 2.12.

From Figure 2.13, we can see that the overlapping values of strength at shifted strain rates appear to align well. However, this is by no means an assurance that the data sets are equivalent at these "equivalent" shifted strain rates. To gain further insight into the similarity of the data sets, we choose several sets of data that correspond to the same "equivalent" strain rate. That is, we choose sets that are taken at a variety of different temperatures and strain rates, but that when shifted according to the shift factors we obtained from creep compliance testing (Figure 2.12), the data all correspond to a thermorheologically equivalent shifted strain rate. If these data sets are similar, and governed by a similar failure mechanism, then we would expect the Weibull distribution of each of these data sets to be similar as well.

We make the assumption that the distribution of fiber strengths can be described by a two-parameter Weibull distribution, where the probability of failure of a fiber is given as a

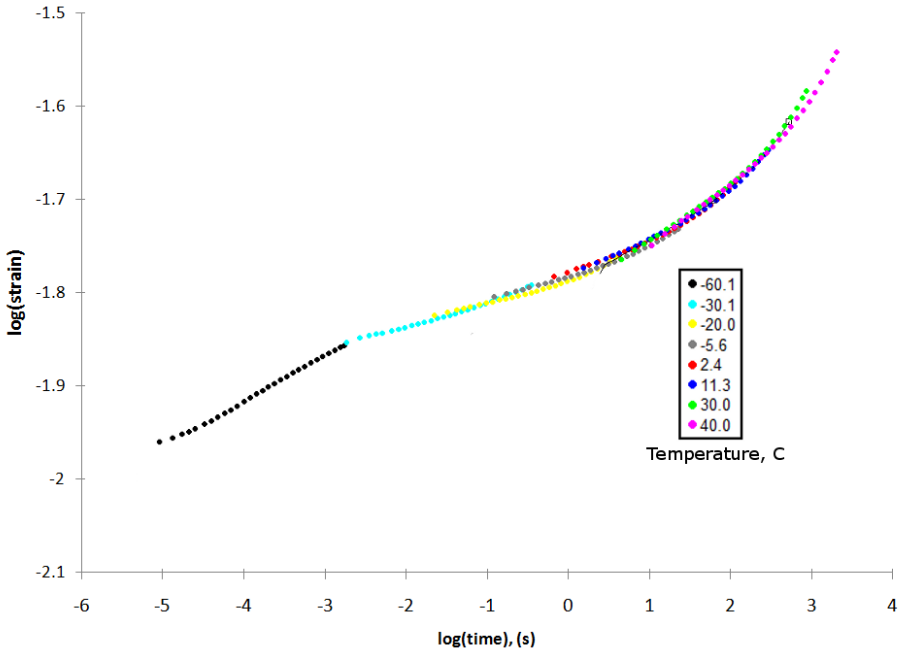

Figure 2.11: Creep compliance master curve for S3000 material.

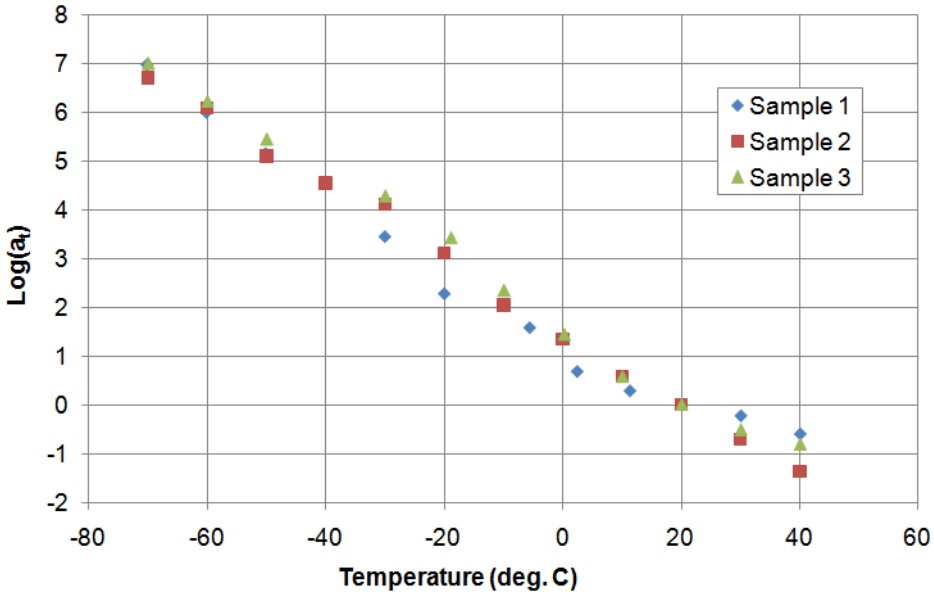

Figure 2.12: S3000 shift factor plot from creep compliance.

function of the fiber length and applied stress

$$P_f = 1 - exp\left[-\frac{L}{L_0}\left(\frac{\sigma}{\sigma_0}\right)^m\right] \tag{2.3}$$

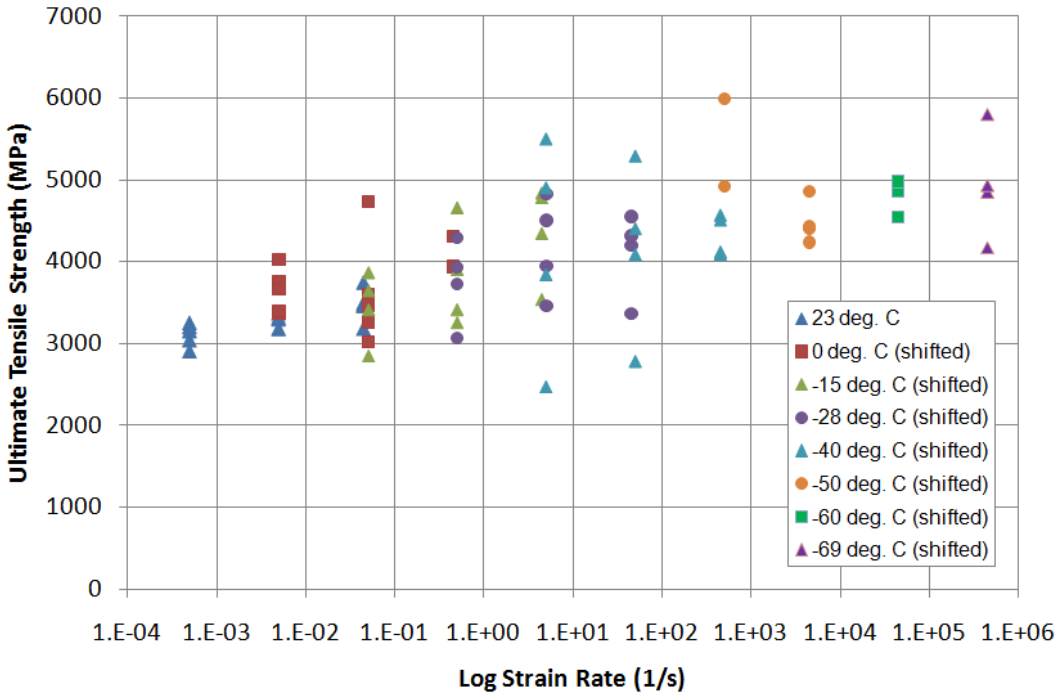

Figure 2.13: S3000 fiber strength shifted according to shift factors from Figure 2.12.

where m is the Weibull modulus, L and L_0 are the sample length and reference length, respectively, and σ and σ_0 are the applied stress and Weibull characteristic strength, respectively. For tests performed at a constant gauge length, we let $L = L_0$ and linearize Equation 2.3 as

$$ln\left(ln\left[\frac{1}{1-P_f}\right]\right) = mln\left(\sigma\right) - mln\left(\sigma_0\right) \tag{2.4}$$

We estimate the probability of failure using Bernard's approximation to median rank

$$P_f^{(i)} = \frac{i - 0.3}{N + 0.4} \tag{2.5}$$

where N is the number of samples and i is the failure order rank. We can then determine m and σ_0 through linear regression.

Figure 2.14 shows the Weibull distribution for three different thermorheologically equivalent strain rates. One data set was recorded at 23 °C and 0.045 sec^{-1}, one at 0 °C and 0.005 sec^{-1}, and one at -15 °C and 0.0005 sec^{-1}. When shifted to 23 °C, each of these data sets corresponds to an equivalent strain rate of 0.045 sec^{-1}. For these three sets, we can see that the Weibull moduli are 9.56, 6.21, and 8.84, respectively. There is some variability in the Weibull distribution. To test the similarity of the distributions, we perform an analysis of covariance with the null hypothesis that set number does not affect slope and intercept. The

analysis yields a P-value of 0.374, indicating that the null hypothesis cannot be rejected. Therefore, we cannot say that the three Weibull distributions are different.

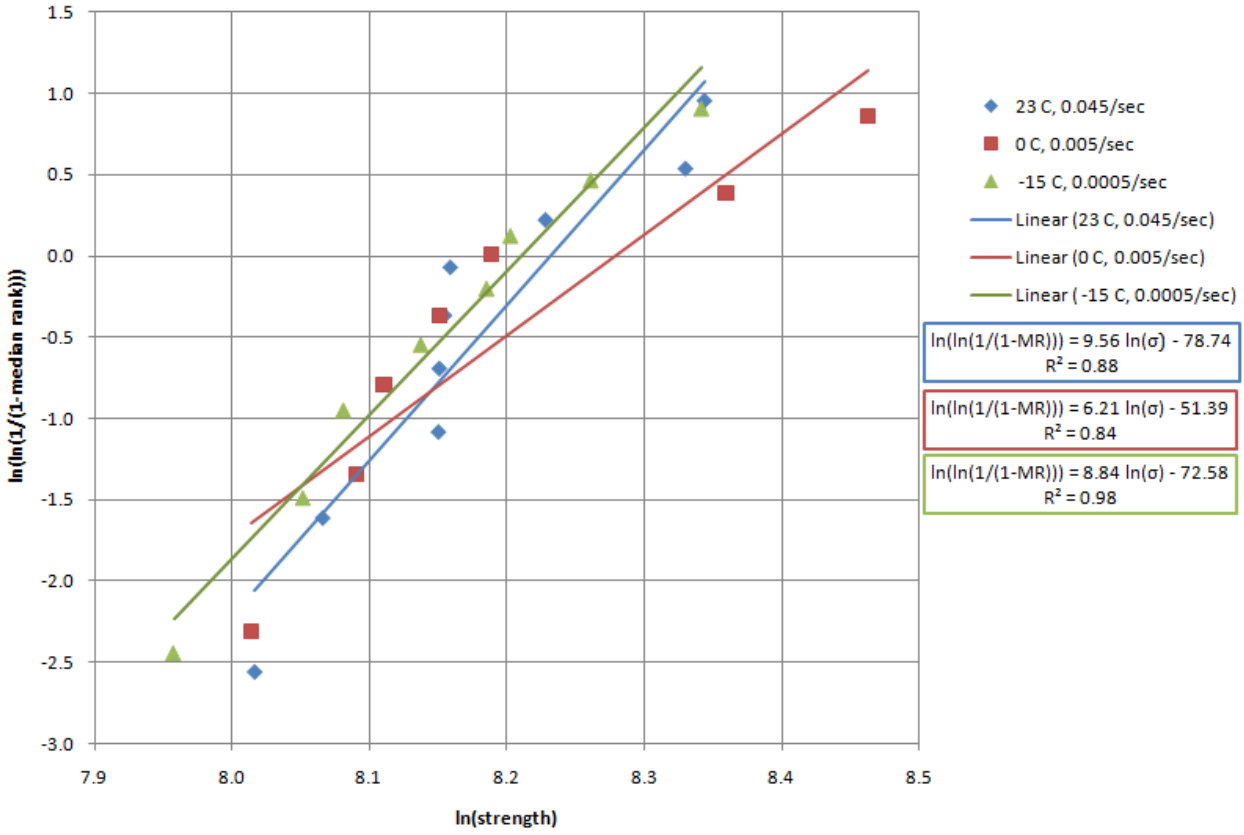

Figure 2.14: Weibull distribution of S3000 fiber strength at three thermorheologically "equivalent" strain rates.

Using Weibull distribution information it is useful to compare the measured fiber strength to lamina tensile strength data for UHMWPE S3000 fiber-based lamina. To accomplish this, a simple bundle strength approximation is used, since the matrix stiffness is orders of magnitude lower than the fiber stiffness. If we assume linear elasticity, we can write

$$\epsilon = \frac{\sigma}{E} \tag{2.6}$$

We can define the reliability as

$$R = 1 - P_f = exp\left[-\frac{L}{L_0}\left(\frac{\epsilon}{\epsilon_0}\right)^m\right] \tag{2.7}$$

thus, the average stress in the fiber bundle at a given strain is

$$\sigma = E_f \epsilon R \tag{2.8}$$

and can thus write the stress in a bulk composite as

$$X_t = V_f E_f \epsilon_0 \left(\frac{L_0}{mLe} \right)^{\frac{1}{m}} \tag{2.9}$$

where V_f is the fiber volume fraction of the composite and E_f is the fiber elastic modulus. From Equations 2.8 and 2.9 we can compare ultimate composite stress with ultimate fiber stress.

In 2009, Cook studied unidirectional lamina based on S3000 fiber [4]. Figure 2.15 shows the bundle strength predicted stress-strain curve based upon a Weibull distribution from Equation 2.8 of a set of S3000 fiber tests at a strain rate of 0.45 sec^{-1} with a fiber volume fraction of 0.7. Figure 2.16 compares this bundle strength prediction to lamina data obtained by Cook.

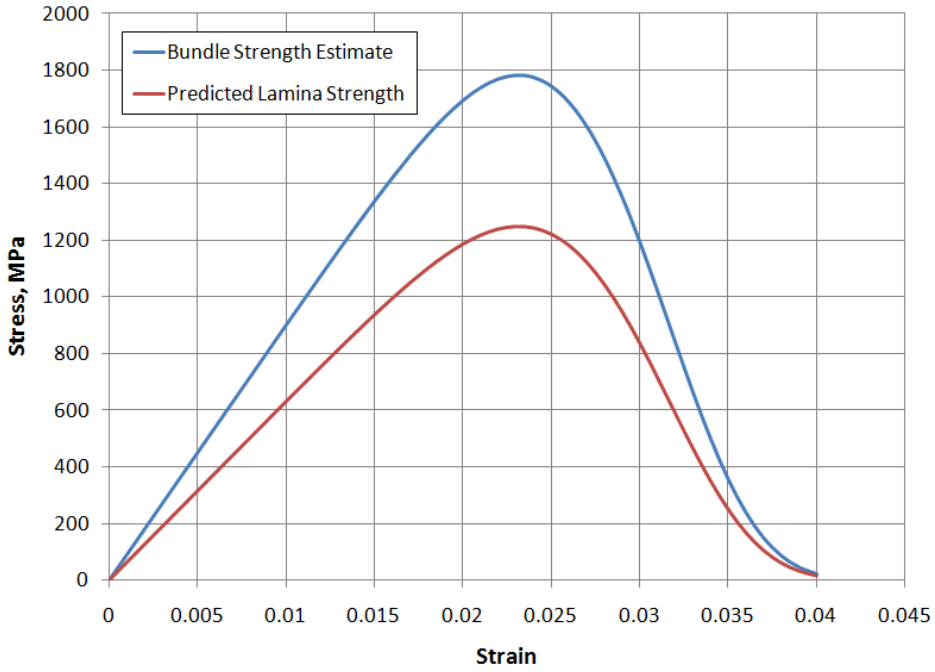

Figure 2.15: Bundle strength predicted stress-strain curve for a strain rate of 0.45 sec^{-1}.

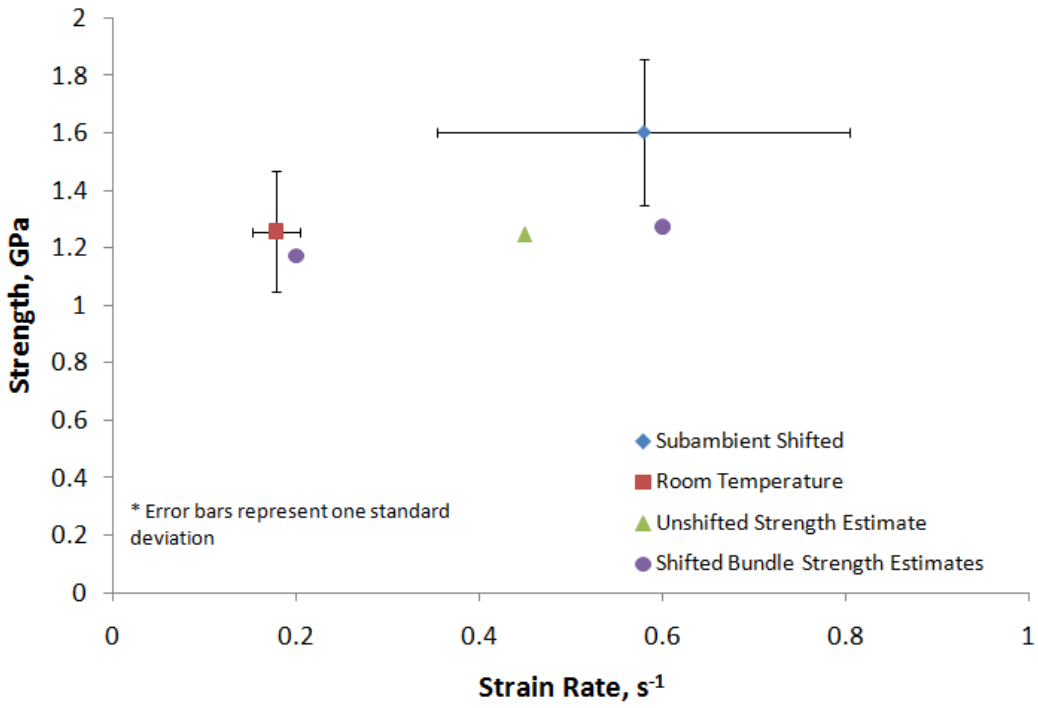

Figure 2.16: Comparison of bundle strength estimate to S3000 lamina data [4].

2.6 Discussion

There are several sources of uncertainty in the fiber tensile testing that was carried out. The largest source of uncertainty resulted from the use of crosshead displacement as the source of strain data. As previously discussed, there was much difficulty in reliably gripping single fibers for testing. Bonding fibers to paper tabs was almost completely unsuccessful. Wrapping fibers around adhesive mandrels was a much more effective solution, in that it allowed sufficient load to be applied to cause fiber failure. However, since the mandrel wrapping approach relies on both adhesion and friction to hold the sample, there was some slipping of the fiber during some tests as the fiber tightened around the cardboard mandrel. As a result, a large uncertainty is generated in strain. Since samples were loaded in displacement control, in terms of strain rate, this slipping of the sample generated some uncertainty in strain rate measurements. This would, of course, affect the data presented in Figures 2.9 and 2.13. However, we remain confident in the behavior of the data since we are spanning 3 decades of "true" strain rate at each temperature, and slipping of the sample in the grips was typically a few percent. Nonetheless, this does contribute to the uncertainty of our strain rate measurement.

Similarly, the lack of confidence in strain measurement made it difficult to present modulus and strain at failure as a function of (shifted) strain rate. The cumulative effect of slipping during a tensile test has a larger effect on strain at failure than it does on instantaneous strain rate at any time during the test. Similarly, since modulus is computed in an average sense from stress and strain, this same cumulative effect of sample slipping renders modulus values as a function of (shifted) strain rate difficult to obtain with the methods presented herein.

It would be preferable to have a source of strain measurement that does not depend on grip integrity, such as an extensometer. However, typical fiber diameter is on the order of 27 μm, making mechanical extensometers impossible. An optical type measurement, such as a laser extensometer would be possible, but the current setup with the Q800 DMA has very little clearance inside the thermal chamber (less than 10 mm), making it difficult to install any sort of measuring device.

Another notable source of uncertainty in the measurements was the variation in fiber shape and cross section area. Figure 2.17 shows an environmental scanning electron microscope (ESEM) image at 380x magnification of a bundle of S3000 fibers. There are several notable characteristics of the fibers as shown in this image. First, it is immediately obvious that fiber cross section area is non-uniform and non-constant between fibers. Second, the cross section shape is non-uniform and non-constant between fibers, and finally, there are "kinking" defects visible along fibers that have been bent. The fibers in this image have been intentionally bent to show the kinking damage, as well as to show fibers from several different angles in the same view. Extreme care was taken in fiber handling to avoid bending and kinking the fibers during processing and testing. However, there is no way to avoid the variation in fiber

cross section area. Since the fibers ultimate application is as part of a composite, it may be appropriate to think of the fiber cross section area in an average sense. As a result, a nominal fiber cross section area was computed in two ways: first by optical methods using the ESEM, and second by an approach using the average mass of a known length of tow with a known number of fibers. Both measurement methods arrived at the same average cross section. The nominal cross section area is 594 μm^2, equivalent to a diameter of 27.5 μm for a round cross section.

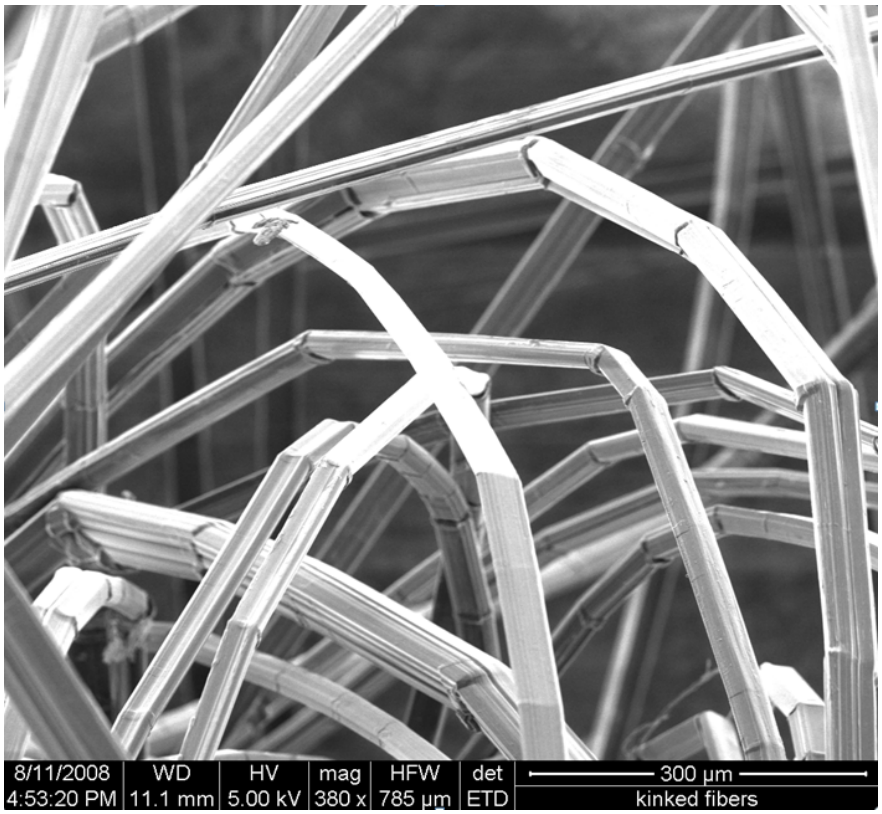

Figure 2.17: ESEM image at 380x magnification of S3000 fibers.

This variation in cross section adds to the overall uncertainty and scatter in the data, since given the number of tests performed, it is not feasible to measure each fiber cross section in an SEM prior to testing. Additionally, fibers bunched and kinked after testing, rendering post-test measurement impossible. Understanding this, we use the nominal fiber cross section area to analyze our test data, compensating for the increased scatter with an increased pool size.

Another source of uncertainty arises from our shifting of creep compliance data to create master curves. As previously discussed, the tTSP method is only strictly applicable for fully amorphous polymers. The UHMWPE fibers that are studied here are a more complex

material system [1]. Therefore, we cannot claim beyond any doubt that the tTSP method we have applied here is valid. Rather, we can only assert that shifted strain rate data appears to be valid, and analysis of the Weibull distributions of ultimate strength at thermorheologically equivalent temperature and strain rates to not contradict this assertion. Additionally, we are shifting test data to strain rates many orders of magnitude larger than the rates at which they were acquired, likely resulting in significant error. Despite the multiple uncertainty sources, we see that data compares favorably to tensile tests on unidirectional lamina tests performed by others, as shown in Figure 2.16.

2.7 Conclusions

Using the method of time-temperature superposition certainly shows promise as a method for estimating material properties outside the range of easily achievable laboratory tests. There are many sources of uncertainty and difficulty in testing this material system. This investigation only scratches the surface of understanding the rate and temperature dependent tensile properties of UHMWPE fibers. In the future, it is recommended that a more precise, reliable method for measuring strain be adopted, possibly using different test equipment. This would allow the metrics of investigation to include modulus and strain at failure as a function of (shifted) strain rate, in addition to ultimate strength.

Additionally, it is recommended that a larger data set be developed for this material system, due to the large scatter generated from the experimental uncertainties previously discussed. There are no "red flags" present in the analysis to date, but a larger data set can further increase confidence in the results of this investigation. Furthermore, a feasible technique should be developed to allow measurement of each fiber prior to testing, thereby greatly decreasing the uncertainty in the data due to fiber cross section area variation.

An alternative method to reduce uncertainty and scatter in the data, with the added benefit of providing an intermediate modeling verification step would be to perform similar testing on fiber tows rather than individual fibers. This alternative would likely come with its own set of challenges and problems, but the corollary study would provide interesting insight nonetheless.

In order to obtain direct comparison to data shifted using tTSP, it would be beneficial for data to be directly measured at high strain rate using another test method, perhaps a Split-Hopkinson bar. This applies to both the fiber data presented herein and the lamina data to which we compare.

Chapter 3

Through Thickness Shear Behavior of UHMWPE Composites

3.1 Abstract

Through-thickness shear response of ultra high molecular weight polyethylene (UHMWPE) composites is of interest to support computational modeling of phenomena such as impact damage. In this study, we attempt to explain a trend of increasing apparent ultimate shear stress with decreased sample thickness. Punch shear testing of UHMWPE composites is conducted to examine the effect of membrane-type behavior on apparent shear strength. Two test fixtures – one allowing, and one preventing backplane curvature – are used in conjunction with finite element modeling to investigate changes in the stress state under punch shear loading and the resulting change in apparent shear strength with sample thickness.

3.2 Introduction

UHMWPE composites are used in many applications requiring light weight and high impact strength, particularly armor applications. One of the most widely used UHMWPE material system is the Spectra/SpectraShield line, manufactured by Honeywell. One of the major applications for these material systems are lightweight ballistic armors. Through-thickness shear properties have been identified as playing a significant role in overall laminate behavior during an impact event [2], [6].

Much work has been done to characterize the properties of laminates in terms of their energy absorption via a punch type test. Gama and Gillespie studied the relation between quasi-static punch-shear behavior and ballistic penetration models for thick section S-2 glass composites [6]. They found that different span to punch ratios (SPR) change the mechanics

of failure. SPR close to 1 leads to shear dominated failure, while large support spans lead to bending dominated failure. In 2005, Xiao et al. studied delamination damage in S-2 glass composites due to punch-shear loading [16]. In both of these cases, the supported diameter is substantially larger than the punch diameter, leading to a significant mix of bending and shear.

In order to support modeling efforts, it is desired to understand the through-thickness shear behavior of UHMWPE composites in terms of material properties. While any physical test is always a measurement of a mechanical system property rather than a true material property, it is desired to isolate the through-thickness shear behavior inasmuch as is possible. In 1995, Liu and Piggott studied the shear properties of polymers and fiber composites [8]. Liu and Piggott used ASTM standard D732-85 as a basis for evaluating shear properties of thermoplastic polymers as well as several epoxy matrix materials. They concluded that the punch shear test may have problems associated with friction between the punch and die, as well as problems developing a stress state close to pure shear, rather than a tension-dominated state. They note these possible issues as sources of uncertainty, but do not suggest a preferred alternative test method.

In this paper, the through-thickness shear properties of Honeywell SpectraShield UHMWPE composites are investigated experimentally. Two test configurations are studied as they relate to apparent shear strength, and an effort is made to explain discrepancies in apparent shear strength as a function of laminate thickness.

3.3 Materials

3.3.1 Laminate Processing Procedure

Samples tested were commercially available Honeywell SpectraShield 1214 product. Either 4 or 8 layers of SpectraShield 1214, each having a lay-up of $[0,90]_2$ were combined to form laminates of lay-up $[0,90]_4$ or $[0,90]_8$. Sheets of the SpectraShield product were cut into approximately 30.5 cm x 30.5 cm panels using a CNC cutting table. Sheets were stacked in the aforementioned configuration. Multiple sheets were pressed in one cycle, with a sheet of silicone coated paper between each. The stack of panels was placed between two 0.635 cm thick smooth aluminum sheets and placed in a hot press. Panels were pressed at a temperature of 118°C and pressure of 19 MPa for 15 minutes. The pressure was removed and the panel was allowed to cool in the press for approximately 15 minutes before being removed. These pressed plates were clamped between rigid fiberglass plates and cut into 50 mm x 50 mm samples using a wet saw. Samples were sufficiently large that cut edges were far away from the punch area. Figure 3.1 shows SpectraShield samples before and after testing. Typical sample thicknesses were 0.53 mm and 1.04 mm, for 8 and 16 layer samples, respectively. Typical fiber volume fractions range from 70 to 75%.

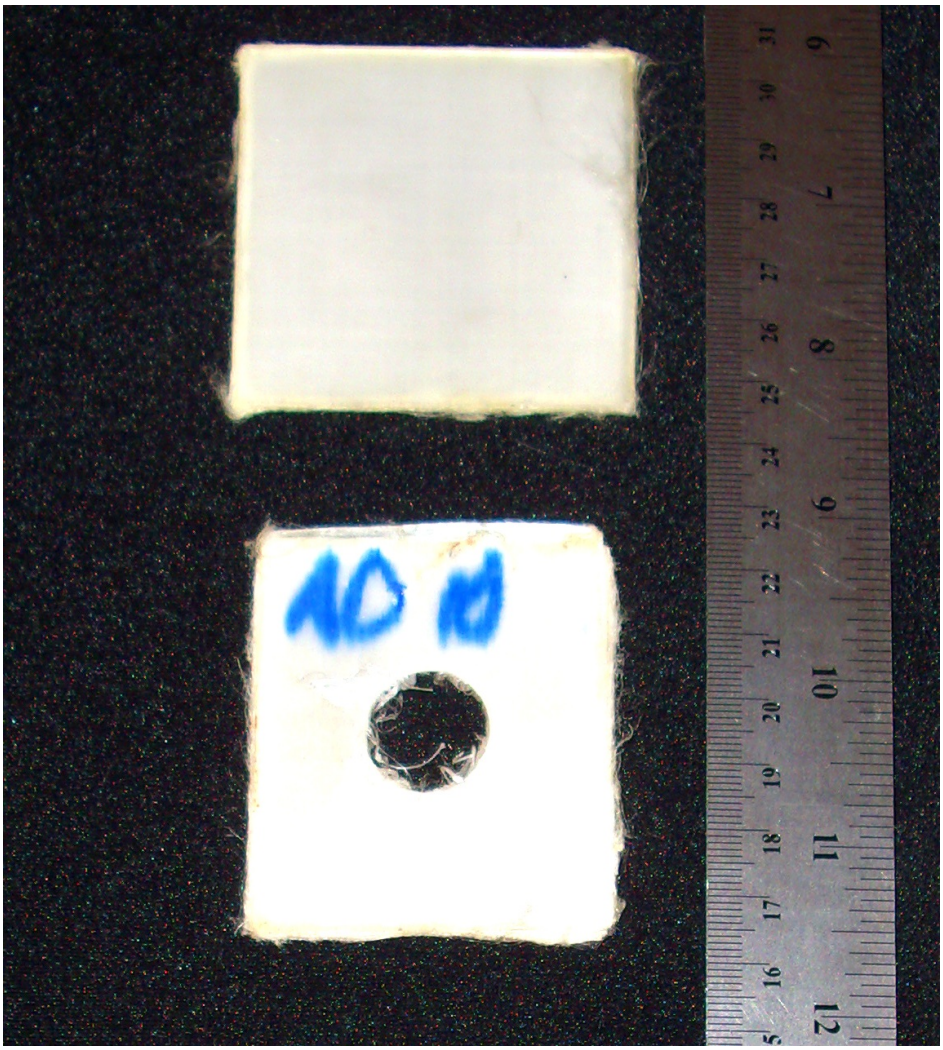

Figure 3.1: SS1214 laminate samples before and after testing.

3.4 Testing Procedure

Specimens were tested using an in-house punch shear assembly. The test setup is similar to ASTM D732-85, but with smaller dimensions to achieve failure within a desired load range based on load frame specifications and predicted strength.

3.4.1 Punch Shear Test Apparatus

The in-house punch-shear assembly consists of a two piece rigid steel die with a 19.05 mm diameter hole through which an 19.00 mm diameter punch is pressed. Thin samples are

clamped in between the two die halves. The punch to die fit is 0.025 mm nominal radius, effectively minimizing the unsupported span of the sample during testing. Laminate thickness is 25 to 50 times this clearance. The goal is to create a region of intense through-thickness shear in the test specimen at the punch/die interface, while minimizing other mechanics phenomena such as bending. Figures 3.2 and 3.3 show the assembly. Up to eight $\frac{1}{2}$-20 inch bolts are used to provide clamping pressure to the specimen. The entire assembly was manufactured out of A2 tool steel and then air-hardened to approximately Rockwell C50 to minimize wear on the edge of the hole at the punch-die-sample interface.

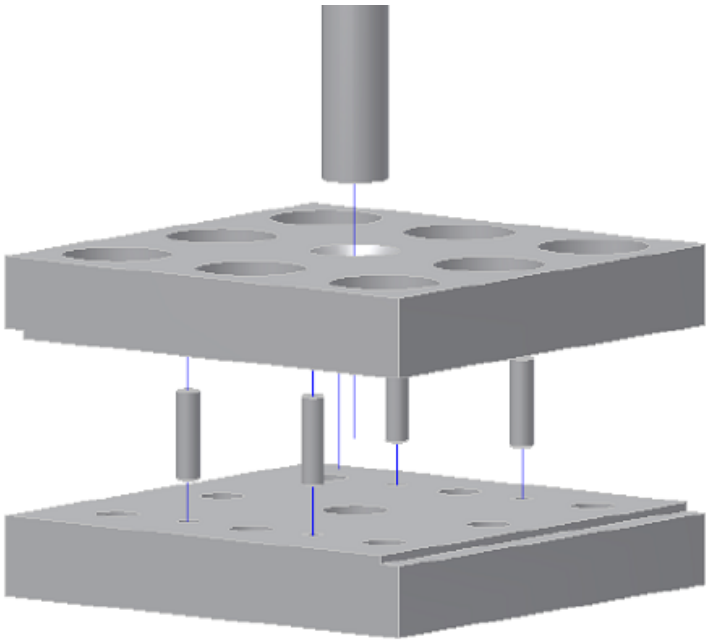

Figure 3.2: Punch shear test apparatus exploded assembly.

3.4.2 Punch Configurations

Two main punch configurations were considered; one allowing and one preventing curvature of the sample during testing. It was hypothesized that disallowing curvature of the sample during testing would create a stress state closer to pure shear, and thereby more effectively decouple tensile and shear modes of failure.

Unsupported Punch

The unsupported punch was simply a right circular cylinder of diameter 19.00 mm and a length of 50 mm. The punch was intended to create a region of intense shear in the sample

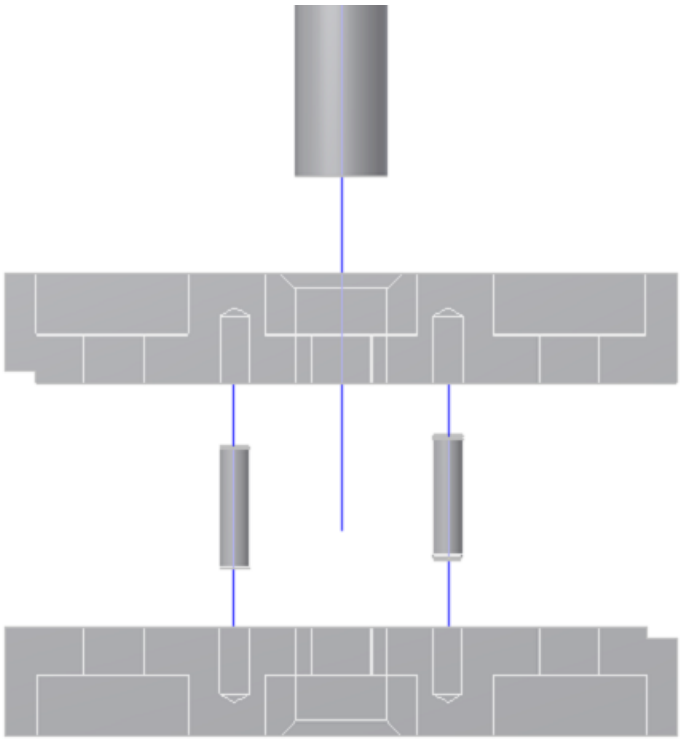

Figure 3.3: Side view of punch shear test apparatus exploded assembly.

at the punch-die interface. The punch was manufactured from A2 tool steel and then air-hardened to approximately Rockwell C50 to minimize wear of the punch edge. Additionally, the face of the punch was surface ground to make the edge as square as possible to reduce bending at the punch-die interface. Figure 3.4 shows the punch used.

Supported Punch

The supported punch was designed to prevent curvature of the sample during testing. The main body of the punch was a right circular cylinder of diameter 19.00 mm and a length of 50 mm. One end of the punch was drilled and tapped with a $\frac{1}{4}$-20 inch hole and surface ground to create a square edge. A second right circular cylinder was machined with a 19.00 mm diameter and a 10 mm length with a 6.35 mm diameter hole through the center to form the clamp. Both pieces were fabricated from A2 tool steel and air-hardened to Rockwell C50, as before. Figure 3.5 shows the assembled punch.

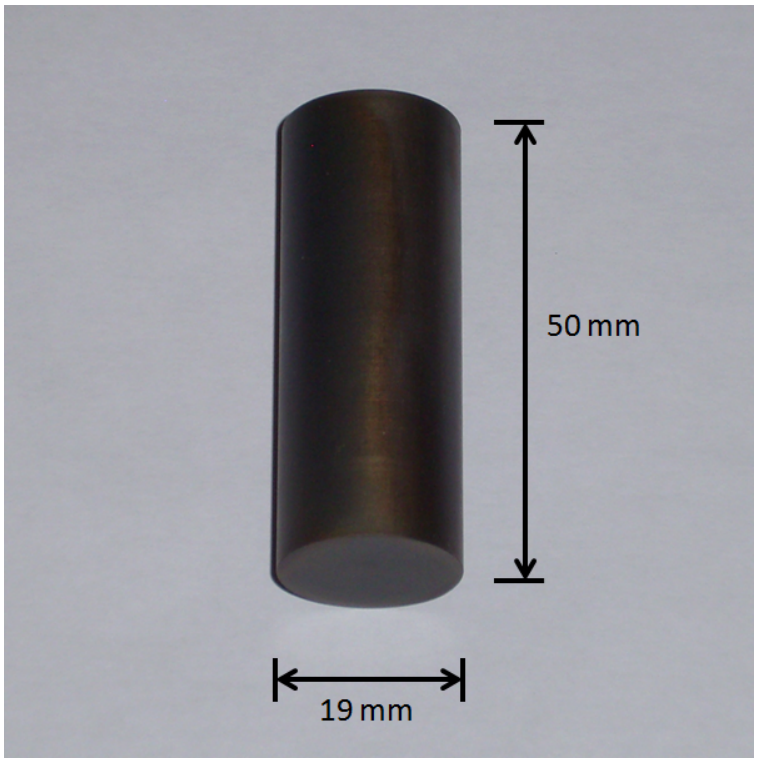

Figure 3.4: Unsupported shear punch fabricated from A2 tool steel.

3.4.3 Punch Shear Test Procedure

Samples of size 50 mm x 50 mm were centered on the bottom portion of the die assembly. A 5 mm diameter hole was cut using a razor blade for samples tested with the supported punch. The top die section was installed. Proper alignment of the holes in the upper and lower section of the die was achieved via pressed dowel pins. Four $\frac{1}{2}$-20 inch bolts were inserted in the bolt holes located at the corners of the die halves and tightened to a torque of 68 N-m. The die assembly was designed with eight bolt holes due to anticipated problems with satisfactorily gripping the samples, however four bolts proved to be sufficient to achieve the necessary grip pressure on the sample to prevent slipping, based upon post-test inspection.

Punch shear testing was conducted in an MTS hydraulic load frame. An 88-kN capacity MTS Force Transducer 661.20 load cell was used to measure load. Displacement measurements were taken from the load frame stroke transducer. An aluminum block was clamped in the upper MTS 647 Hydraulic Wedge Grip and used to transfer load to the punch head. Control and data collection was provided using an in-house National Instruments (NI) LabVIEW program. The punch shear test assembly was rested on the lower grip frame, which was verified to be parallel to the aluminum block in the upper grip to ensure load was applied vertically and did not cause the punch to jam in the die assembly. Figure 3.6 shows the

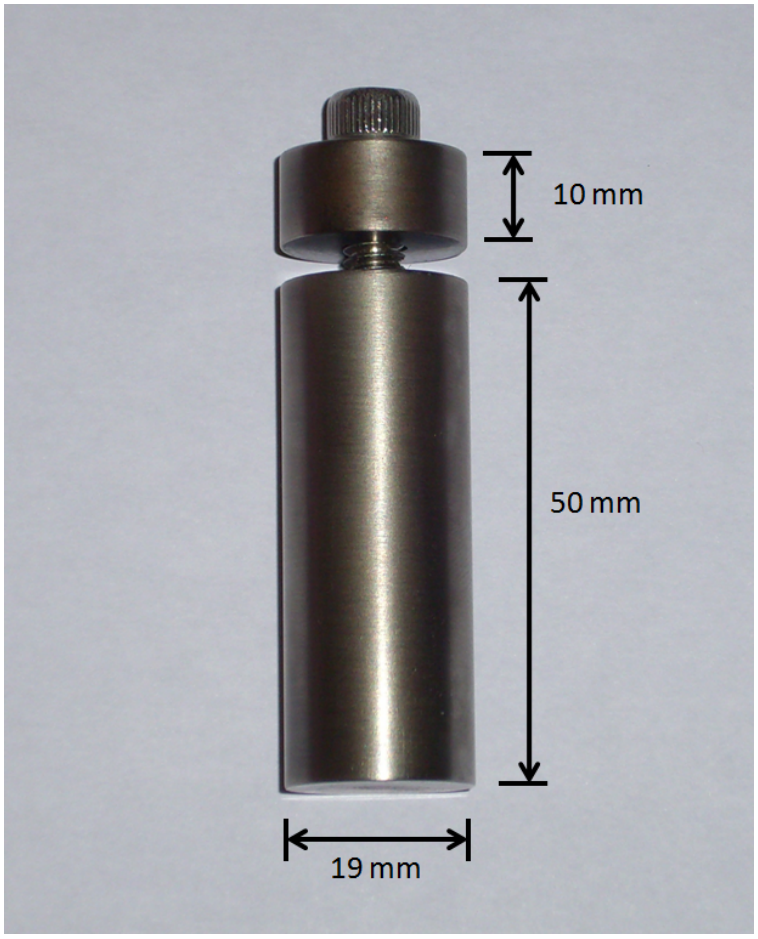

Figure 3.5: Supported shear punch fabricated from A2 tool steel.

assembled test apparatus in the load frame prior to a typical test.

Tests were conducted in load control at a load rate of 667 $\frac{N}{sec}$. Load and displacement channels were recorded at 50 Hz using the in-house NI LabVIEW program. After each test, the punch was removed, die halves unbolted, and the sample removed for inspection of the failure surface.

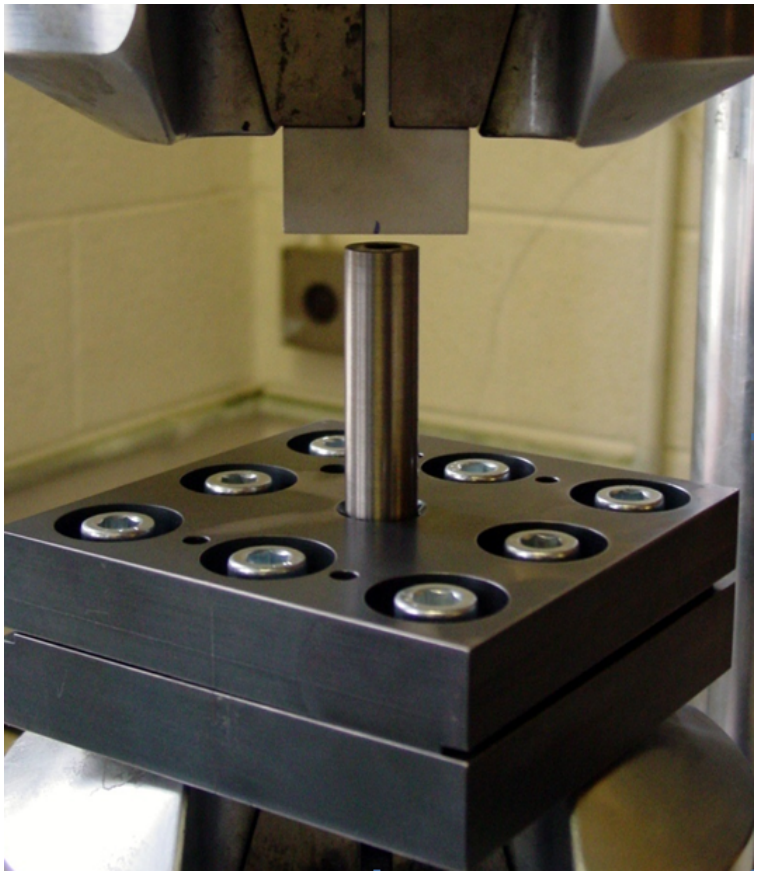

Figure 3.6: Assembled punch shear test apparatus in MTS hydraulic load frame.

3.5 Finite Element Modeling

Recognizing that the cross-ply laminate construction cannot be represented with an axisymmetric model, and given the fact that many of the necessary material properties are unknown, an isotropic, linear elastic material model is used, solely for the purpose of investigating the nature of the deformation and stresses in the test specimen. The intention of this model is not to gather exact, nor even quantitative representation of the problem, but rather gain insight into the comparative representation of each of the test types conducted. The four models are tabulated in Table 3.1. The load applied in each case corresponds to approximately 5% of the failure load for the unsupported punch case for that thickness.

An axisymmetric finite element (FE) model representing a simplified version of the physical tests was developed using ABAQUS 6.9-2. Die halves and both punch types were modeled in order to utilize contact loading to study the deformation of the sample. Mapped meshes of 4-noded linear quadrilateral (Q4) elements were used for the model. Meshes were refined for convergence of stress and displacement away from the singularity at the interface of the sample and jig. The outside edge of the model was fixed, representing the rest of the die assembly as rigid. Axisymmetry boundary conditions were applied at the axis of revolution, and a pressure load was applied to the top of the punch. For two cases representing the supported punch, an additional body was modeled to constrain the curvature of the specimen.

Table 3.1: FE model case summary.

Model	Sample Thickness	Punch Type
1	8 Layers	Unsupported
2	8 Layers	Supported
3	16 Layers	Unsupported
4	16 Layers	Supported

3.6 Results

3.6.1 Punch Shear Testing

For this test geometry, through-thickness shear stress is ideally represented as

$$\tau = \frac{F}{A_{shear}} \tag{3.1}$$

where A_{shear} is defined as

$$A_{shear} = \pi D_p t \tag{3.2}$$

where D_p is the average of the punch and die diameters and t is the sample thickness.

The results for ultimate shear stress versus sample thickness are shown in Figure 3.7. Average ultimate shear stress for each thickness and punch type are given in Table 3.2. Additionally, standard deviation and coefficient of variation (COV) for each data set is shown in Table 3.3.

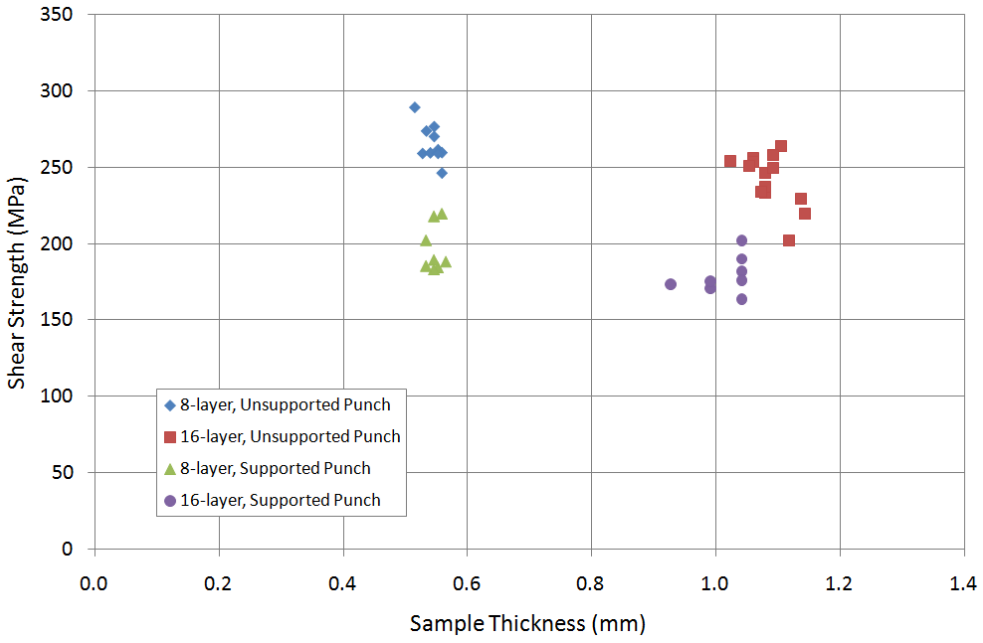

Figure 3.7: Ultimate shear stress versus thickness.

Typical load-displacement curves for unsupported punch samples are given in Figure 3.8. We note that there is a distinct slope change for both 8 and 16 layer samples. Similarly,

Table 3.2: Average ultimate shear strength and deviation for supported and unsupported punch types (MPa).

	Unsupported	Supported
8-layer	266	196
16-layer	242	179
Absolute Difference	24	17
Percent Difference	9.0	8.7

Table 3.3: Standard deviation and COV for supported and unsupported punch types.

		Unsupported	Supported
8-layer	Std. Dev. (MPa)	12.1	15.1
	COV (%)	4.6	7.7
16-layer	Std. Dev. (MPa)	17.1	12.2
	COV (%)	7.1	6.8

Figure 3.9 shows typical load-displacement curves for samples tested using the supported punch.

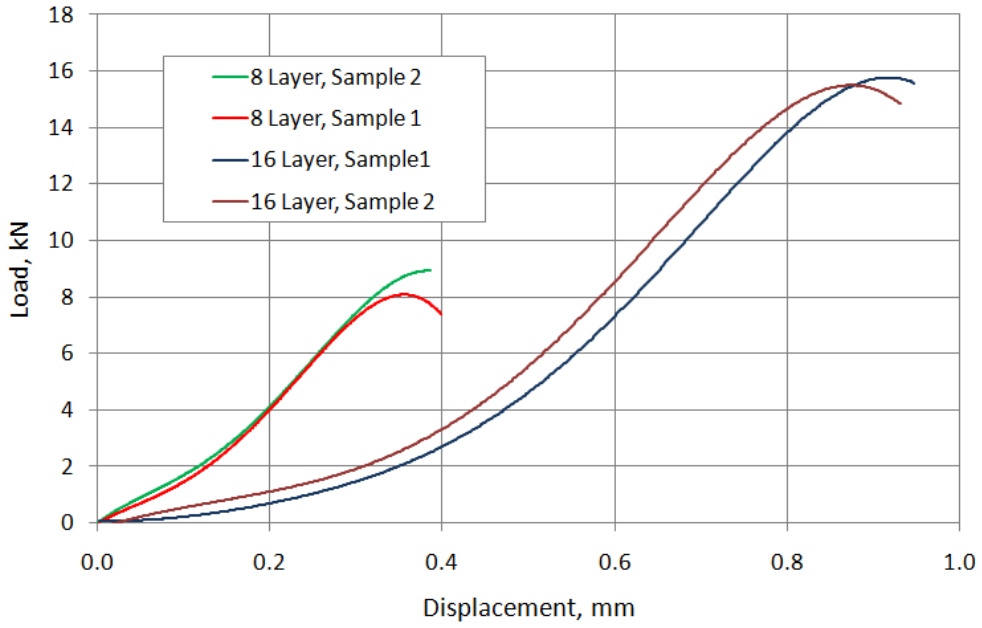

Figure 3.8: Load versus displacement for selected unsupported punch samples.

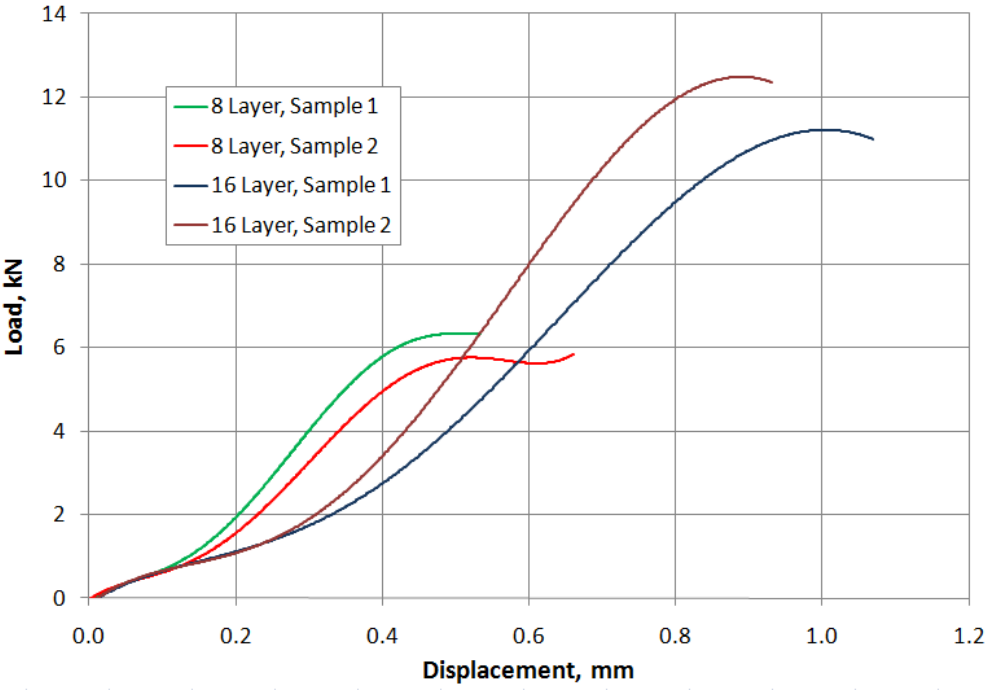

Figure 3.9: Load versus displacement for selected supported punch samples.

3.6.2 Finite Element Modeling

The FE solution for each of the four test cases (as tabulated in Table 3.1) was computed using ABAQUS 6.9-2. Figure 3.10 shows the through-thickness shear stress distribution for an 8-layer laminate loaded with the unsupported punch configuration. From Figure 3.11 it can be seen that a small zone of concentrated shear stress exists near the punch-die interface. Figure 3.12 shows the in-plane radial stress distribution. The radial stress in the laminate is an order of magnitude lower than the shear stress.

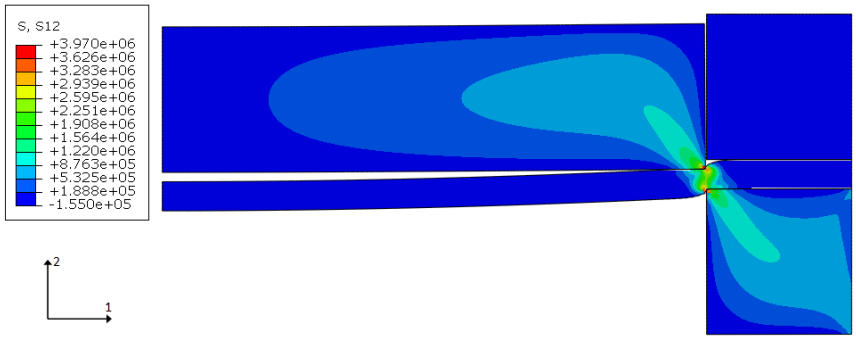

Figure 3.10: Through thickness shear of 8-layer panel with unsupported punch (Pa).

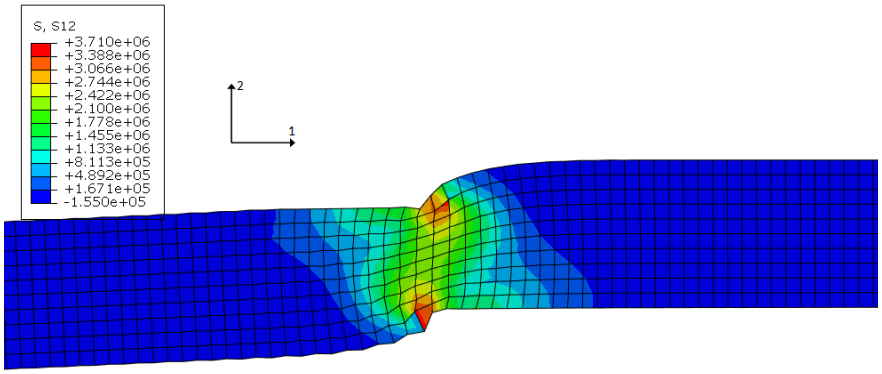

Figure 3.11: Through thickness shear of 8-layer panel with unsupported punch (Pa).

For the case of the 8-layer panel loaded with the supported punch, the through-thickness shear stress distribution is shown in Figure 3.13. Figure 3.14 shows the same shear stress distribution at our area of interest. Figure 3.15 shows the radial stress in the panel. Again, the radial stress is an order of magnitude lower than the shear stress.

For the case of the 16-layer panel loaded with the unsupported punch, the through-thickness shear stress distribution is shown in Figure 3.16. Figure 3.17 shows the same shear stress

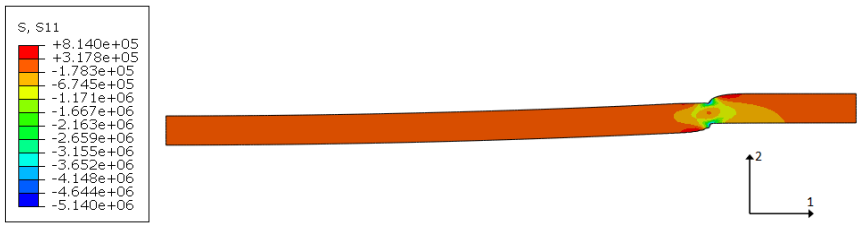

Figure 3.12: Radial stress of 8-layer panel with unsupported punch (Pa).

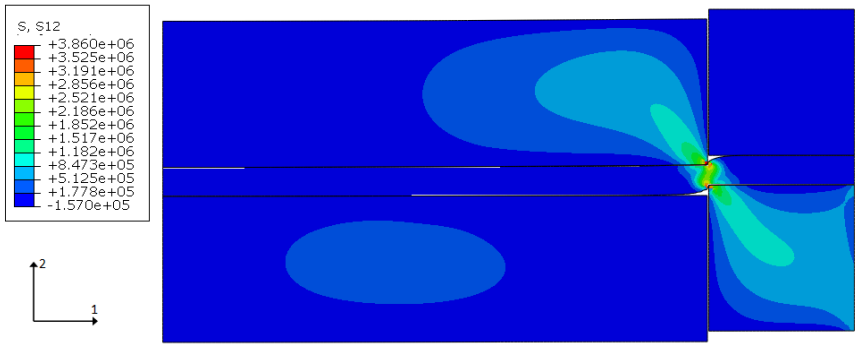

Figure 3.13: Through thickness shear of 8-layer panel with supported punch (Pa).

distribution at our area of interest. Figure 3.18 shows the radial stress in the panel. Again, the radial stress is an order of magnitude lower than the shear stress.

For the case of the 16-layer panel loaded with the supported punch, the through-thickness shear stress distribution is shown in Figure 3.19. Figure 3.20 shows the same shear stress

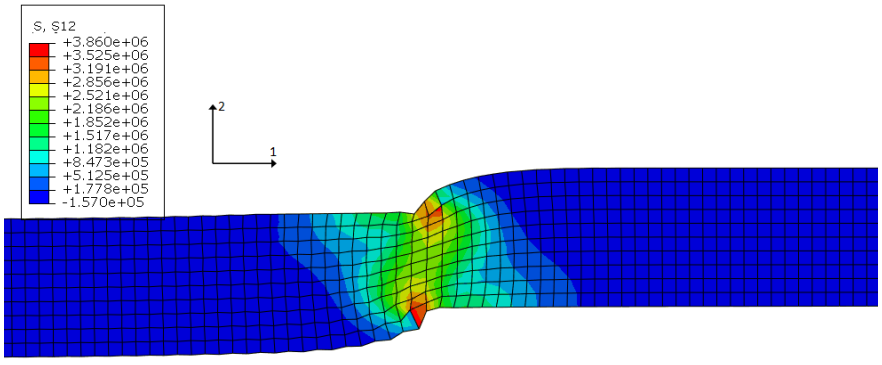

Figure 3.14: Through thickness shear of 8-layer panel with supported punch (Pa).

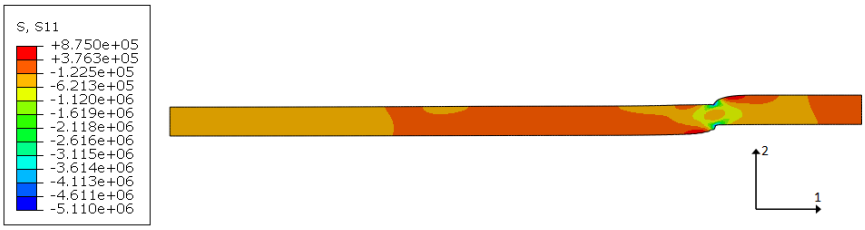

Figure 3.15: Radial stress of 8-layer panel with supported punch (Pa).

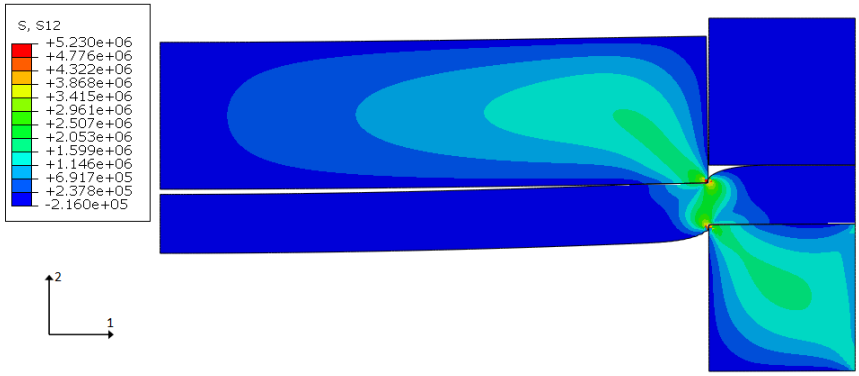

Figure 3.16: Through thickness shear of 16-layer panel with unsupported punch (Pa).

distribution at our area of interest. Figure 3.21 shows the radial stress in the panel. Again, the radial stress is an order of magnitude lower than the shear stress.

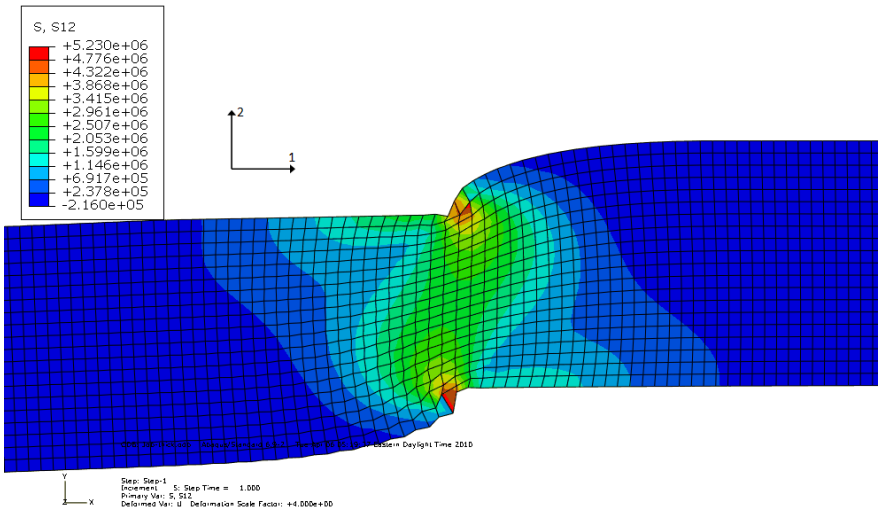

Figure 3.17: Through thickness shear of 16-layer panel with unsupported punch (Pa).

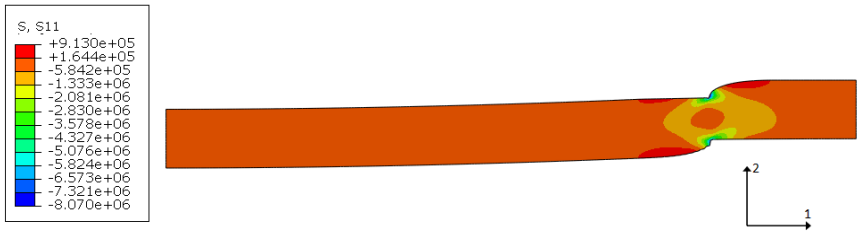

Figure 3.18: Radial stress of 16-layer panel with unsupported punch (Pa).

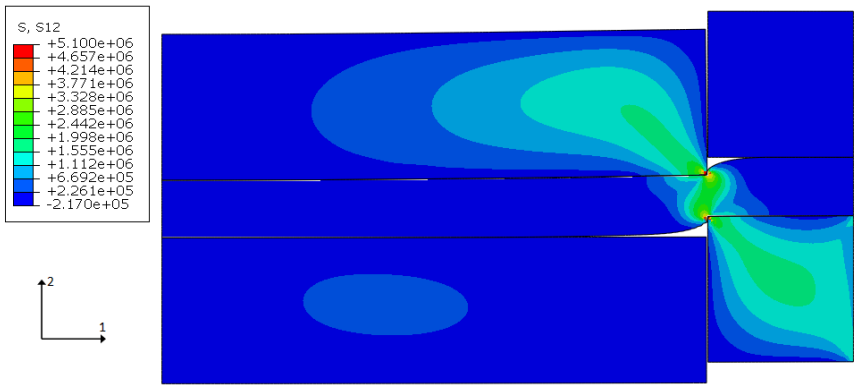

Figure 3.19: Through thickness shear of 16-layer panel with supported punch (Pa).

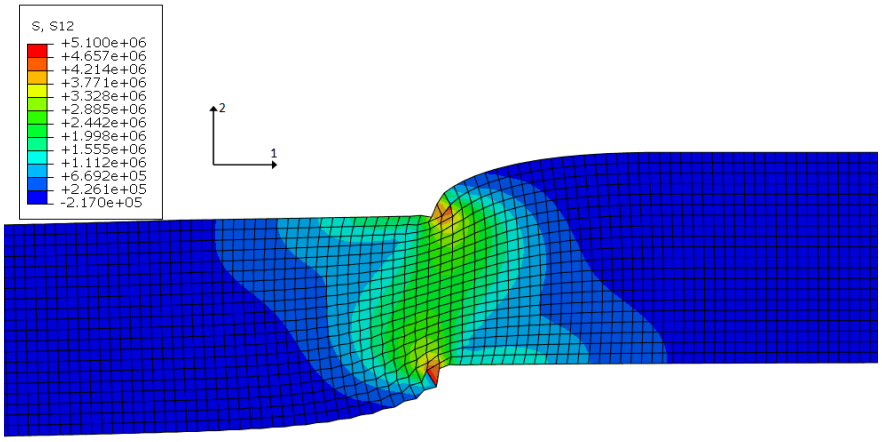

Figure 3.20: Through thickness shear of 16-layer panel with supported punch (Pa).

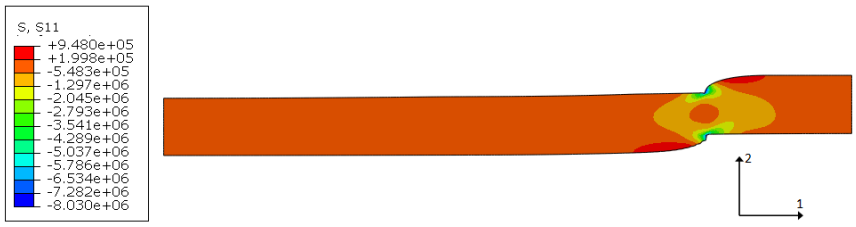

Figure 3.21: Radial stress of 16-layer panel-with supported punch (Pa).

3.7 Discussion

There appears to be a trend of increased apparent shear strength with decreasing thickness. If the state of stress was truly pure shear through the thickness of the sample, apparent shear strength would not be expected to vary with specimen thickness. Initially, when only unsupported punch tests had been performed, it was hypothesized that this increase in apparent strength was due to a membrane type behavior. Thinner 8-layer samples have less bending stiffness and more ability to rotate when compared to 16-layer samples, given the constant clearance in the punch and die geometry. It stands to reason that apparent shear strength would then be higher for samples that are experiencing more of a membrane type state of stress, due to the extreme anisotropy of UHMWPE fibers that comprise the SpectraShield laminates.

This notion is further supported by the distinct change in slope of the load-displacement curves shown in Figures 3.8 and 3.9. It is possible that the increase in slope during the course of the punch shear test is due to a nonlinear geometric effect that is governed by a membrane type behavior. The same phenomenon that governs this increased mechanical stiffness could be governing the increase in observed shear strength.

It was initially expected that the supported punch that prevented curvature of the sample would reduce this hypothesized membrane behavior and would result in apparent shear strengths that were more consistent versus sample thickness. However, given the results in Figure 3.7 and Tables 3.2 and 3.3, this does not appear to be the case. For both supported and unsupported punch types, an 8 to 9 percent decrease in apparent shear strength is observed with a two fold increase in sample thickness.

In retrospect, the design of the supported punch clamp does not provide the same clamping pressure ability as the die assembly. For the tests in this research, clamping pressure on the sample is estimated to be approximately 6 MPa. In contrast, the estimated clamping pressure that can be achieved on the punch clamp is approximately 1 MPa. In retrospect, a better punch design with a fine threaded fastener would be a better choice to allow for equal clamping pressure in the punch and die sections.

It is also possible that this difference in apparent shear strength with thickness is the result of the clearance between the punch and die. Radial clearance is only 0.025 mm, which approaches the limit of a slip fit, however average diameter of a single fiber is 0.0275 mm. It is possible that instead of being loaded in true shear, the weak matrix material is deforming and allowing fibers to rotate and follow the edge of the punch rather than shearing as anticipated. A punch with tighter tolerances could perhaps be manufactured, but binding of the punch and die may become an issue.

The simple FE model representation of the problem does not indicate that a substantial membrane component is present in the state of stress. However, this model is a very simplistic representation of the problem, and many unknowns remain. Material properties are

not properly represented (nor are they well known). Phenomena such as localized plastic deformation near the punch-die interface are not represented. Additionally, properties such as friction are not known in the test configuration under consideration. A fully developed finite element model of this complex problem is outside the scope of this thesis.

3.8 Conclusions

In general, the results were repeatable, with a coefficient of variation of well less than 10%. It is important to note that the properties measured in this research represent mechanical properties related to the particular test geometry, not true material properties. One of the ultimate goals of this research is to estimate true material properties based upon results of these tests. Resolving the apparent difference in ultimate shear strength is a critical step to this end.

It was originally hypothesized that the change in apparent shear strength was due to an increase in membrane type behavior in thinner samples, artificially increasing the apparent through-thickness shear strength. Initial investigation of the problem does not appear to support this hypothesis. Possible improvements to the test method include a better punch design allowing greater clamping pressure, as well as a smaller clearance between the punch and die. It is suggested that both of these avenues be pursued in future research. Additional future work should be conducted to expand and improve the finite element representation of the test problem, better representing the materials and boundary conditions.

Chapter 4

Conclusions

There is much left to be studied to fully understand the response of both UHMWPE composites and their constituents. The research presented in this thesis attempts to aid in an understanding of the behavior of this material system, in terms of both state of stress and the strain rate. There is perpetually more work to be done in the field.

4.1 Time-Temperature Superposition and High Rate Response of UHMWPE Fibers

This research discusses the development of a method for conducting repeatable tests of UHMWPE tensile strength. Creep compliance testing was discussed as a method for generating factors for shifting strength plots with strain rate and temperature. The applicability of these creep compliance shift factors to strength data was investigated. No evidence was found to suggest that creep compliance shift factors are not applicable to fiber tensile strength in this case for this material system. There are several sources of uncertainty in this method, the most notable of which is the method by which strain is measured. Possible future investigations and recommendations for improvement to this method were discussed.

It would be desirable as a corollary to this work to conduct fiber tests on this material system using a Split Hopkinson Bar setup (or other high strain rate test setup) to validate the predictions made in this research. However, without this validation, the general trends exhibited in the data are consistent with the behavior that is expected with temperature and strain rate.

4.2 Through Thickness Shear Behavior of UHMWPE Composites

Possible reasons for variation in apparent ultimate through-thickness shear strength are investigated in this research. Through physical testing of laminate through-thickness properties, along with development of a very basic finite element model, the apparent through-thickness shear strength is investigated. The original hypothesis of a membrane type behavior contributing to the difference in apparent shear strengths does not appear to be directly supported by the test results thus far. This is an area where future work should be conducted, as the behavior of UHMWPE laminates in this mode is not well understood.

4.3 Future Work

There is much work that remains in order to completely understand and determine the constitutive behavior of UHMWPE composites and constituents as a function of temperature and strain rate.

The application of the tTSP method to fiber tensile strength testing can be extended to include modulus and strain at failure as a function of temperature and (shifted) strain rate. The implementation of a test method including more precise strain measurement that does not rely on grip integrity along with a more reliable method of gripping fibers could greatly improve the data pool.

Additionally, expansion of the investigation to include testing of fiber tows could help alleviate some of the uncertainty issues encountered with nonuniform fiber cross section size and shape. The comparison of these two types of data sets could offer valuable insight into the problem at hand and offer an intermediate step for model verification between fiber and lamina/laminate levels of complexity.

Laminate through-thickness shear properties should be further investigated with one or more improved test apparatus designs. Additionally, more than two laminate layup configurations and thicknesses should be investigated. The basic finite element model should be improved to better represent the material properties and mechanics of the problem.

Furthermore, since through-thickness shear properties are of interest to support modeling of impact type events, the rate dependence of shear properties should be investigated as well. The method of strain rate extrapolation using tTSP discussed in Chapter 2 should be investigated as it relates to through-thickness shear. However, it should be noted that the work in Chapter 2 was conducted on fiber alone, while the laminate is a two-part material system. The applicability of tTSP needs to be investigated to ensure that it is appropriate for use in predicting rate-dependent shear response.

Bibliography

[1] Alcock B., Cabrera N.O., Barkoula N.M., Reynolds C.T., Govaert L.E., Peijs T. The effect of temperature and strain rate on the mechanical properties of highly oriented polypropylene tapes and all-polypropylene composites. *Composites Science and Technology*, 67:20612070, 2007.

[2] Bhatnagar, A. *Lightweight ballistic composites: military and law-enforcement applications*. Woodhead, 2006.

[3] Brinson H., Brinson L. *Polymer engineering science and viscoelasticity*. Springer, 2008.

[4] Cook, F.P. Characterization of uhmwpe laminates for high strain rate applications. *Virginia Polytechnic Institute and State University*, 2010.

[5] Feih, S., Thraner A., Lilholt, H. Tensile strength and fracture surface characterisation of sized and unsized glass fibers. *Journal of Materials Science*, 40:1615–1623, 2005.

[6] Gama, B.A., Gillespie, J.W. Punch shear based penetration model of ballistic impact of thick-section composites. *Composite Structures*, 86:356–369, 2008.

[7] Gu, B. Analytical modeling for the ballistic perforation of planar plain-woven fabric taret by projectile. *Composites Science and Technology*, 34:361–371, 2003.

[8] Liu, K, Piggott, M. Shear strength of polymers and fibre composites: 1. thermoplastic and thermoset polymers. *Composites*, 26(12):829–840, 1995. doi: 10.1016/0010-4361(95)90876-2.

[9] Miyano Y., Nakada M., Naoyuki S. Accelerated testing for long-term durability of gfrp laminates for marine use. *Composites: Part B*, 35:497–502, 2004.

[10] Peijs, T., et al. Role of interface and fibre anisotropy in controlling the performance of polyethylene-fibre-reinforced composites. *Composites Science and Technology*, 52: 449–466, 1994.

[11] Scharfeld, T., D'Arrigo C. A single hair fiber tesnsile tester for operation under a scanning electron microscope. 2004.

[12] Shim, V., Tan, V. Modelling deformation and damage characteristics of woven fabric under small projectile impact. *International Journal of Impact Engineering*, 16:585–605, 1995.

[13] Tan, V.B.C., Ching T.W. Computational simulation of fabric armour subjected to ballistic impacts. *International Journal of Impact Engineering*, 32:1737–1751, 2006.

[14] Tan V.B.C., Zeng X.S. Characterization and constitutive modeling of aramid fibers at high strain rates. *International Journal of Impact Engineering*, 32:1737–1751, 2006.

[15] Wang, Y., Zia, Y. The effects of strain rate on the mechanical behaviour of kevlar fiber bundles: an experimental and theoretical study. *Composites Science and Technology*, 1998.

[16] Xiao, J., Gama, B., Gillespie Jr., J. Progressive damage and delamination in plain weave s-2 glass/sc-15 composites under quasi-static punch-shear loading. *Composite Structures*, 78:182–196, 2007.

Content Licenses

SPRINGER LICENSE
TERMS AND CONDITIONS

Apr 26, 2010

This is a License Agreement between Pierce D Umberger ("You") and Springer ("Springer") provided by Copyright Clearance Center ("CCC"). The license consists of your order details, the terms and conditions provided by Springer, and the payment terms and conditions.

All payments must be made in full to CCC. For payment instructions, please see information listed at the bottom of this form.

License Number	2416560836769
License date	Apr 26, 2010
Licensed content publisher	Springer
Licensed content publication	Journal of Materials Science (full set)
Licensed content title	Tensile strength and fracture surface characterisation of sized and unsized glass fibers
Licensed content author	S. Feih
Licensed content date	Apr 1, 2005
Volume number	40
Issue number	7
Type of Use	Thesis/Dissertation
Portion	Figures
Author of this Springer article	No
Order reference number	
Title of your thesis / dissertation	Characterization and Response of Thermoplastic Composites and Constituents
Expected completion date	Apr 2010
Estimated size(pages)	54
Total	0.00 USD
Terms and Conditions	

Introduction
The publisher for this copyrighted material is Springer Science + Business Media. By clicking "accept" in connection with completing this licensing transaction, you agree that the following terms and conditions apply to this transaction (along with the Billing and Payment terms and conditions established by Copyright Clearance Center, Inc. ("CCC"), at the time that you opened your Rightslink account and that are available at any time at http://myaccount.copyright.com).

Limited License
With reference to your request to reprint in your thesis material on which Springer Science and Business Media control the copyright, permission is granted, free of charge, for the use indicated in your enquiry. Licenses are for one-time use only with a maximum distribution equal to the number that you identified in the licensing process.

This License includes use in an electronic form, provided it is password protected or on the university's intranet, destined to microfilming by UMI and University repository. For any other electronic use, please contact Springer at (permissions.dordrecht@springer.com or permissions.heidelberg@springer.com)

The material can only be used for the purpose of defending your thesis, and with a maximum of 100 extra copies in paper.

Although Springer holds copyright to the material and is entitled to negotiate on rights, this license is only valid, provided permission is also obtained from the (co) author (address is given with the article/chapter) and provided it concerns original material which does not

carry references to other sources (if material in question appears with credit to another source, authorization from that source is required as well). Permission free of charge on this occasion does not prejudice any rights we might have to charge for reproduction of our copyrighted material in the future.

Altering/Modifying Material: Not Permitted
However figures and illustrations may be altered minimally to serve your work. Any other abbreviations, additions, deletions and/or any other alterations shall be made only with prior written authorization of the author(s) and/or Springer Science + Business Media. (Please contact Springer at permissions.dordrecht@springer.com or permissions.heidelberg@springer.com)

Reservation of Rights
Springer Science + Business Media reserves all rights not specifically granted in the combination of (i) the license details provided by you and accepted in the course of this licensing transaction, (ii) these terms and conditions and (iii) CCC's Billing and Payment terms and conditions.

Copyright Notice:
Please include the following copyright citation referencing the publication in which the material was originally published. Where wording is within brackets, please include verbatim.
"With kind permission from Springer Science+Business Media: <book/journal title, chapter/article title, volume, year of publication, page, name(s) of author(s), figure number(s), and any original (first) copyright notice displayed with material>."

Warranties: Springer Science + Business Media makes no representations or warranties with respect to the licensed material.

Indemnity
You hereby indemnify and agree to hold harmless Springer Science + Business Media and CCC, and their respective officers, directors, employees and agents, from and against any and all claims arising out of your use of the licensed material other than as specifically authorized pursuant to this license.

No Transfer of License
This license is personal to you and may not be sublicensed, assigned, or transferred by you to any other person without Springer Science + Business Media's written permission.

No Amendment Except in Writing
This license may not be amended except in a writing signed by both parties (or, in the case of Springer Science + Business Media, by CCC on Springer Science + Business Media's behalf).

Objection to Contrary Terms
Springer Science + Business Media hereby objects to any terms contained in any purchase order, acknowledgment, check endorsement or other writing prepared by you, which terms are inconsistent with these terms and conditions or CCC's Billing and Payment terms and conditions. These terms and conditions, together with CCC's Billing and Payment terms and conditions (which are incorporated herein), comprise the entire agreement between you and Springer Science + Business Media (and CCC) concerning this licensing transaction. In the event of any conflict between your obligations established by these terms and conditions and those established by CCC's Billing and Payment terms and conditions, these terms and conditions shall control.

Jurisdiction
All disputes that may arise in connection with this present License, or the breach thereof, shall be settled exclusively by the country's law in which the work was originally published.

Other terms and conditions:

v1.2

Gratis licenses (referencing $0 in the Total field) are free. Please retain this printable license for your reference. No payment is required.

If you would like to pay for this license now, please remit this license along with your payment made payable to "COPYRIGHT CLEARANCE CENTER" otherwise you will be invoiced within 48 hours of the license date. Payment should be in the form of a check or money order referencing your account number and this invoice number RLNK10774083.
Once you receive your invoice for this order, you may pay your invoice by credit card. Please follow instructions provided at that time.

Make Payment To:
Copyright Clearance Center
Dept 001
P.O. Box 843006
Boston, MA 02284-3006

If you find copyrighted material related to this license will not be used and wish to cancel, please contact us referencing this license number 2416560836769 and noting the reason for cancellation.

Questions? customercare@copyright.com or +1-877-622-5543 (toll free in the US) or +1-978-646-2777.

ELSEVIER LICENSE
TERMS AND CONDITIONS

Apr 26, 2010

This is a License Agreement between Pierce D Umberger ("You") and Elsevier ("Elsevier") provided by Copyright Clearance Center ("CCC"). The license consists of your order details, the terms and conditions provided by Elsevier, and the payment terms and conditions.

All payments must be made in full to CCC. For payment instructions, please see information listed at the bottom of this form.

Supplier	Elsevier Limited The Boulevard,Langford Lane Kidlington,Oxford,OX5 1GB,UK
Registered Company Number	1982084
Customer name	Pierce D Umberger
Customer address	Engineering Science and Mechanics Blacksburg, VA 24061
License Number	2416561358693
License date	Apr 26, 2010
Licensed content publisher	Elsevier
Licensed content publication	International Journal of Impact Engineering
Licensed content title	Characterization and constitutive modeling of aramid fibers at high strain rates
Licensed content author	V.B.C. Tan, X.S. Zeng, V.P.W. Shim
Licensed content date	November 2008
Volume number	35
Issue number	11
Pages	11
Type of Use	Thesis / Dissertation
Portion	Figures/tables/illustrations
Number of Figures/tables/illustrations	1
Format	Both print and electronic
You are an author of the Elsevier article	No
Are you translating?	No
Order Reference Number	
Expected publication date	Apr 2010
Elsevier VAT number	GB 494 6272 12
Permissions price	0.00 USD
Value added tax 0.0%	0.00 USD
Total	0.00 USD
Terms and Conditions	

INTRODUCTION

1. The publisher for this copyrighted material is Elsevier. By clicking "accept" in connection with completing this licensing transaction, you agree that the following terms and conditions apply to this transaction (along with the Billing and Payment terms and conditions

established by Copyright Clearance Center, Inc. ("CCC"), at the time that you opened your Rightslink account and that are available at any time at http://myaccount.copyright.com).

GENERAL TERMS

2. Elsevier hereby grants you permission to reproduce the aforementioned material subject to the terms and conditions indicated.

3. Acknowledgement: If any part of the material to be used (for example, figures) has appeared in our publication with credit or acknowledgement to another source, permission must also be sought from that source. If such permission is not obtained then that material may not be included in your publication/copies. Suitable acknowledgement to the source must be made, either as a footnote or in a reference list at the end of your publication, as follows:

"Reprinted from Publication title, Vol /edition number, Author(s), Title of article / title of chapter, Pages No., Copyright (Year), with permission from Elsevier [OR APPLICABLE SOCIETY COPYRIGHT OWNER]." Also Lancet special credit - "Reprinted from The Lancet, Vol. number, Author(s), Title of article, Pages No., Copyright (Year), with permission from Elsevier."

4. Reproduction of this material is confined to the purpose and/or media for which permission is hereby given.

5. Altering/Modifying Material: Not Permitted. However figures and illustrations may be altered/adapted minimally to serve your work. Any other abbreviations, additions, deletions and/or any other alterations shall be made only with prior written authorization of Elsevier Ltd. (Please contact Elsevier at permissions@elsevier.com)

6. If the permission fee for the requested use of our material is waived in this instance, please be advised that your future requests for Elsevier materials may attract a fee.

7. Reservation of Rights: Publisher reserves all rights not specifically granted in the combination of (i) the license details provided by you and accepted in the course of this licensing transaction, (ii) these terms and conditions and (iii) CCC's Billing and Payment terms and conditions.

8. License Contingent Upon Payment: While you may exercise the rights licensed immediately upon issuance of the license at the end of the licensing process for the transaction, provided that you have disclosed complete and accurate details of your proposed use, no license is finally effective unless and until full payment is received from you (either by publisher or by CCC) as provided in CCC's Billing and Payment terms and conditions. If full payment is not received on a timely basis, then any license preliminarily granted shall be deemed automatically revoked and shall be void as if never granted. Further, in the event that you breach any of these terms and conditions or any of CCC's Billing and Payment terms and conditions, the license is automatically revoked and shall be void as if never granted. Use of materials as described in a revoked license, as well as any use of the materials beyond the scope of an unrevoked license, may constitute copyright infringement and publisher reserves the right to take any and all action to protect its copyright in the materials.

9. Warranties: Publisher makes no representations or warranties with respect to the licensed material.

10. Indemnity: You hereby indemnify and agree to hold harmless publisher and CCC, and their respective officers, directors, employees and agents, from and against any and all claims arising out of your use of the licensed material other than as specifically authorized pursuant to this license.

11. No Transfer of License: This license is personal to you and may not be sublicensed, assigned, or transferred by you to any other person without publisher's written permission.

12. No Amendment Except in Writing: This license may not be amended except in a writing signed by both parties (or, in the case of publisher, by CCC on publisher's behalf).

13. Objection to Contrary Terms: Publisher hereby objects to any terms contained in any purchase order, acknowledgment, check endorsement or other writing prepared by you, which terms are inconsistent with these terms and conditions or CCC's Billing and Payment terms and conditions. These terms and conditions, together with CCC's Billing and Payment terms and conditions (which are incorporated herein), comprise the entire agreement between you and publisher (and CCC) concerning this licensing transaction. In the event of any conflict between your obligations established by these terms and conditions and those established by CCC's Billing and Payment terms and conditions, these terms and conditions shall control.

14. Revocation: Elsevier or Copyright Clearance Center may deny the permissions described in this License at their sole discretion, for any reason or no reason, with a full refund payable to you. Notice of such denial will be made using the contact information provided by you. Failure to receive such notice will not alter or invalidate the denial. In no event will Elsevier or Copyright Clearance Center be responsible or liable for any costs, expenses or damage incurred by you as a result of a denial of your permission request, other than a refund of the amount(s) paid by you to Elsevier and/or Copyright Clearance Center for denied permissions.

LIMITED LICENSE

The following terms and conditions apply only to specific license types:

15. **Translation**: This permission is granted for non-exclusive world **English** rights only unless your license was granted for translation rights. If you licensed translation rights you may only translate this content into the languages you requested. A professional translator must perform all translations and reproduce the content word for word preserving the integrity of the article. If this license is to re-use 1 or 2 figures then permission is granted for non-exclusive world rights in all languages.

16. **Website**: The following terms and conditions apply to electronic reserve and author websites:
Electronic reserve: If licensed material is to be posted to website, the web site is to be password-protected and made available only to bona fide students registered on a relevant course if:
This license was made in connection with a course,
This permission is granted for 1 year only. You may obtain a license for future website posting,
All content posted to the web site must maintain the copyright information line on the bottom of each image,
A hyper-text must be included to the Homepage of the journal from which you are licensing at http://www.sciencedirect.com/science/journal/xxxxx or the Elsevier homepage for books at http://www.elsevier.com , and
Central Storage: This license does not include permission for a scanned version of the material to be stored in a central repository such as that provided by Heron/XanEdu.

17. **Author website** for journals with the following additional clauses:

All content posted to the web site must maintain the copyright information line on the bottom of each image, and
he permission granted is limited to the personal version of your paper. You are not allowed to download and post the published electronic version of your article (whether PDF or HTML, proof or final version), nor may you scan the printed edition to create an electronic version,
A hyper-text must be included to the Homepage of the journal from which you are licensing at http://www.sciencedirect.com/science/journal/xxxxx , As part of our normal production process, you will receive an e-mail notice when your article appears on Elsevier's online service ScienceDirect (www.sciencedirect.com). That e-mail will include the article's Digital Object Identifier (DOI). This number provides the electronic link to the published article and should be included in the posting of your personal version. We ask that you wait until you receive this e-mail and have the DOI to do any posting.
Central Storage: This license does not include permission for a scanned version of the material to be stored in a central repository such as that provided by Heron/XanEdu.

18. **Author website** for books with the following additional clauses:
Authors are permitted to place a brief summary of their work online only.
A hyper-text must be included to the Elsevier homepage at http://www.elsevier.com

All content posted to the web site must maintain the copyright information line on the bottom of each image
You are not allowed to download and post the published electronic version of your chapter, nor may you scan the printed edition to create an electronic version.
Central Storage: This license does not include permission for a scanned version of the material to be stored in a central repository such as that provided by Heron/XanEdu.

19. **Website** (regular and for author): A hyper-text must be included to the Homepage of the journal from which you are licensing at http://www.sciencedirect.com/science/journal/xxxxx. or for books to the Elsevier homepage at http://www.elsevier.com

20. **Thesis/Dissertation**: If your license is for use in a thesis/dissertation your thesis may be submitted to your institution in either print or electronic form. Should your thesis be published commercially, please reapply for permission. These requirements include permission for the Library and Archives of Canada to supply single copies, on demand, of the complete thesis and include permission for UMI to supply single copies, on demand, of the complete thesis. Should your thesis be published commercially, please reapply for permission.

21. **Other Conditions**: None

v1.6

Gratis licenses (referencing $0 in the Total field) are free. Please retain this printable license for your reference. No payment is required.

If you would like to pay for this license now, please remit this license along with your payment made payable to "COPYRIGHT CLEARANCE CENTER" otherwise you will be invoiced within 48 hours of the license date. Payment should be in the form of a check or money order referencing your account number and this invoice number RLNK10774093.
Once you receive your invoice for this order, you may pay your invoice by credit card. Please follow instructions provided at that time.

Make Payment To:
Copyright Clearance Center
Dept 001
P.O. Box 843006
Boston, MA 02284-3006

If you find copyrighted material related to this license will not be used and wish to cancel, please contact us referencing this license number 2416561358693 and noting the reason for cancellation.

Questions? customercare@copyright.com or +1-877-622-5543 (toll free in the US) or +1-978-646-2777.

ELSEVIER LICENSE
TERMS AND CONDITIONS

Apr 26, 2010

This is a License Agreement between Pierce D Umberger ("You") and Elsevier ("Elsevier") provided by Copyright Clearance Center ("CCC"). The license consists of your order details, the terms and conditions provided by Elsevier, and the payment terms and conditions.

All payments must be made in full to CCC. For payment instructions, please see information listed at the bottom of this form.

Supplier	Elsevier Limited The Boulevard,Langford Lane Kidlington,Oxford,OX5 1GB,UK
Registered Company Number	1982084
Customer name	Pierce D Umberger
Customer address	Engineering Science and Mechanics Blacksburg, VA 24061
License Number	2416561211070
License date	Apr 26, 2010
Licensed content publisher	Elsevier
Licensed content publication	Composites Science and Technology
Licensed content title	The effect of temperature and strain rate on the mechanical properties of highly oriented polypropylene tapes and all-polypropylene composites
Licensed content author	B. Alcock, N.O. Cabrera, N.-M. Barkoula, C.T. Reynolds, L.E. Govaert, T. Peijs
Licensed content date	August 2007
Volume number	67
Issue number	10
Pages	10
Type of Use	Thesis / Dissertation
Portion	Figures/tables/illustrations
Number of Figures/tables/illustrations	2
Format	Both print and electronic
You are an author of the Elsevier article	No
Are you translating?	No
Order Reference Number	
Expected publication date	Apr 2010
Elsevier VAT number	GB 494 6272 12
Permissions price	0.00 USD
Value added tax 0.0%	0.00 USD
Total	0.00 USD
Terms and Conditions	

INTRODUCTION

1. The publisher for this copyrighted material is Elsevier. By clicking "accept" in connection with completing this licensing transaction, you agree that the following terms and conditions apply to this transaction (along with the Billing and Payment terms and conditions established by Copyright Clearance Center, Inc. ("CCC"), at the time that you opened your Rightslink account and that are available at any time at http://myaccount.copyright.com).

GENERAL TERMS

2. Elsevier hereby grants you permission to reproduce the aforementioned material subject to the terms and conditions indicated.

3. Acknowledgement: If any part of the material to be used (for example, figures) has appeared in our publication with credit or acknowledgement to another source, permission must also be sought from that source. If such permission is not obtained then that material may not be included in your publication/copies. Suitable acknowledgement to the source must be made, either as a footnote or in a reference list at the end of your publication, as follows:

"Reprinted from Publication title, Vol /edition number, Author(s), Title of article / title of chapter, Pages No., Copyright (Year), with permission from Elsevier [OR APPLICABLE SOCIETY COPYRIGHT OWNER]." Also Lancet special credit - "Reprinted from The Lancet, Vol. number, Author(s), Title of article, Pages No., Copyright (Year), with permission from Elsevier."

4. Reproduction of this material is confined to the purpose and/or media for which permission is hereby given.

5. Altering/Modifying Material: Not Permitted. However figures and illustrations may be altered/adapted minimally to serve your work. Any other abbreviations, additions, deletions and/or any other alterations shall be made only with prior written authorization of Elsevier Ltd. (Please contact Elsevier at permissions@elsevier.com)

6. If the permission fee for the requested use of our material is waived in this instance, please be advised that your future requests for Elsevier materials may attract a fee.

7. Reservation of Rights: Publisher reserves all rights not specifically granted in the combination of (i) the license details provided by you and accepted in the course of this licensing transaction, (ii) these terms and conditions and (iii) CCC's Billing and Payment terms and conditions.

8. License Contingent Upon Payment: While you may exercise the rights licensed immediately upon issuance of the license at the end of the licensing process for the transaction, provided that you have disclosed complete and accurate details of your proposed use, no license is finally effective unless and until full payment is received from you (either by publisher or by CCC) as provided in CCC's Billing and Payment terms and conditions. If full payment is not received on a timely basis, then any license preliminarily granted shall be deemed automatically revoked and shall be void as if never granted. Further, in the event that you breach any of these terms and conditions or any of CCC's Billing and Payment terms and conditions, the license is automatically revoked and shall be void as if never granted. Use of materials as described in a revoked license, as well as any use of the materials beyond the scope of an unrevoked license, may constitute copyright infringement and publisher reserves the right to take any and all action to protect its copyright in the materials.

9. Warranties: Publisher makes no representations or warranties with respect to the licensed material.

10. Indemnity: You hereby indemnify and agree to hold harmless publisher and CCC, and their respective officers, directors, employees and agents, from and against any and all claims arising out of your use of the licensed material other than as specifically authorized pursuant to this license.

11. No Transfer of License: This license is personal to you and may not be sublicensed, assigned, or transferred by you to any other person without publisher's written permission.

12. No Amendment Except in Writing: This license may not be amended except in a writing signed by both parties (or, in the case of publisher, by CCC on publisher's behalf).

13. Objection to Contrary Terms: Publisher hereby objects to any terms contained in any purchase order, acknowledgment, check endorsement or other writing prepared by you, which terms are inconsistent with these terms and conditions or CCC's Billing and Payment terms and conditions. These terms and conditions, together with CCC's Billing and Payment terms and conditions (which are incorporated herein), comprise the entire agreement between you and publisher (and CCC) concerning this licensing transaction. In the event of any conflict between your obligations established by these terms and conditions and those established by CCC's Billing and Payment terms and conditions, these terms and conditions shall control.

14. Revocation: Elsevier or Copyright Clearance Center may deny the permissions described in this License at their sole discretion, for any reason or no reason, with a full refund payable to you. Notice of such denial will be made using the contact information provided by you. Failure to receive such notice will not alter or invalidate the denial. In no event will Elsevier or Copyright Clearance Center be responsible or liable for any costs, expenses or damage incurred by you as a result of a denial of your permission request, other than a refund of the amount(s) paid by you to Elsevier and/or Copyright Clearance Center for denied permissions.

LIMITED LICENSE

The following terms and conditions apply only to specific license types:

15. **Translation**: This permission is granted for non-exclusive world **English** rights only unless your license was granted for translation rights. If you licensed translation rights you may only translate this content into the languages you requested. A professional translator must perform all translations and reproduce the content word for word preserving the integrity of the article. If this license is to re-use 1 or 2 figures then permission is granted for non-exclusive world rights in all languages.

16. **Website**: The following terms and conditions apply to electronic reserve and author websites:
Electronic reserve: If licensed material is to be posted to website, the web site is to be password-protected and made available only to bona fide students registered on a relevant course if:
This license was made in connection with a course,
This permission is granted for 1 year only. You may obtain a license for future website posting,
All content posted to the web site must maintain the copyright information line on the bottom of each image,
A hyper-text must be included to the Homepage of the journal from which you are licensing at http://www.sciencedirect.com/science/journal/xxxxx or the Elsevier homepage for books at http://www.elsevier.com , and
Central Storage: This license does not include permission for a scanned version of the material to be stored in a central repository such as that provided by Heron/XanEdu.

17. **Author website** for journals with the following additional clauses:

All content posted to the web site must maintain the copyright information line on the bottom of each image, and
he permission granted is limited to the personal version of your paper. You are not allowed to download and post the published electronic version of your article (whether PDF or HTML, proof or final version), nor may you scan the printed edition to create an electronic version,
A hyper-text must be included to the Homepage of the journal from which you are licensing at http://www.sciencedirect.com/science/journal/xxxxx , As part of our normal production process, you will receive an e-mail notice when your article appears on Elsevier's online service ScienceDirect (www.sciencedirect.com). That e-mail will include the article's Digital Object Identifier (DOI). This number provides the electronic link to the published article and should be included in the posting of your personal version. We ask that you wait until you receive this e-mail and have the DOI to do any posting.

Central Storage: This license does not include permission for a scanned version of the material to be stored in a central repository such as that provided by Heron/XanEdu.

18. **Author website** for books with the following additional clauses:
Authors are permitted to place a brief summary of their work online only.
A hyper-text must be included to the Elsevier homepage at http://www.elsevier.com

All content posted to the web site must maintain the copyright information line on the bottom of each image
You are not allowed to download and post the published electronic version of your chapter, nor may you scan the printed edition to create an electronic version.
Central Storage: This license does not include permission for a scanned version of the material to be stored in a central repository such as that provided by Heron/XanEdu.

19. **Website** (regular and for author): A hyper-text must be included to the Homepage of the journal from which you are licensing at http://www.sciencedirect.com/science/journal/xxxxx. or for books to the Elsevier homepage at http://www.elsevier.com

20. **Thesis/Dissertation**: If your license is for use in a thesis/dissertation your thesis may be submitted to your institution in either print or electronic form. Should your thesis be published commercially, please reapply for permission. These requirements include permission for the Library and Archives of Canada to supply single copies, on demand, of the complete thesis and include permission for UMI to supply single copies, on demand, of the complete thesis. Should your thesis be published commercially, please reapply for permission.

21. **Other Conditions**: None

v1.6

Gratis licenses (referencing $0 in the Total field) are free. Please retain this printable license for your reference. No payment is required.

If you would like to pay for this license now, please remit this license along with your payment made payable to "COPYRIGHT CLEARANCE CENTER" otherwise you will be invoiced within 48 hours of the license date. Payment should be in the form of a check or money order referencing your account number and this invoice number RLNK10774091.
Once you receive your invoice for this order, you may pay your invoice by credit card. Please follow instructions provided at that time.

Make Payment To:
Copyright Clearance Center
Dept 001
P.O. Box 843006
Boston, MA 02284-3006

If you find copyrighted material related to this license will not be used and wish to cancel, please contact us referencing this license number 2416561211070 and noting the reason for cancellation.

Questions? customercare@copyright.com or +1-877-622-5543 (toll free in the US) or +1-978-646-2777.